sciendo

Civil and Environmental Engineering
Vol. 21, Issue 2, 1139-1165, DOI: 10.2478/cee-2025-0085

ENHANCED BIOSAND FILTRATION WITH CANE PAPYRUS FOR IMPROVED PHYSICOCHEMICAL AND MICROBIAL CONTAMINANT REMOVAL IN WATER TREATMENT

Ahmed A. JAFFER[1, *], Maad F. AL JUBOURY[1]

[1]Civil Engineering Department, University of Kerbala, 56001 Kerbala, Iraq.
*corresponding author: ahmed.a.jaafer@s.uokerbala.edu.iq

Abstract

This study investigates the removal efficiency of various water contaminants using a Biological Sand Filtration (BSF) system under different operational conditions. The performance of the BSF system was evaluated for microbial contaminants (E. coli), suspended solids, dissolved solids (TDS), electrical conductivity (EC), hardness, chloride (Cl), sulfate (SO_4), and turbidity. Key operational parameters such as pH, retention time, flow rate, and the biological layer thickness were optimized to determine their impact on contaminant removal efficiency. The results demonstrated that a 48-hour retention time achieved complete E. coli removal (100%), while the 2 mm biological layer contributed to a significant reduction in microbial contaminants (81.2%). The highest turbidity reduction (85.4%) was achieved at a 0.5 m/h flow rate, and the pH 4.01 condition optimized the removal of TDS (65.4%) and EC (56.9%). Total hardness removal was maximized at 25°C, while magnesium removal was most effective with a 48-hour retention time (75.2%). Chloride removal peaked at 25°C (73.2%), and sulfate removal was optimized at pH 6.86 (52.9%). The study highlights the importance of adjusting operational parameters to optimize the performance of BSF systems for diverse contaminants, providing a sustainable and efficient solution for water quality improvement. The findings offer valuable insights for designing and operating BSF systems in varying environmental conditions and contribute to the development of cost-effective water treatment technologies.

Keywords:

Biosand filter;
Water purification;
Cane Papyrus;
Microbial removal;
Physicochemical removal;
Contaminant reduction.

1 Introduction

Access to clean and safe drinking water remains a critical challenge worldwide, particularly in developing regions where contamination from industrial discharge, agricultural runoff, and inadequate sanitation infrastructure threatens public health [1,2]. According to the World Health Organization (WHO), waterborne diseases caused by microbial and chemical contamination contribute to millions of deaths annually, with children under the age of five being the most affected [3]. Addressing this challenge requires the development of effective, low-cost, and sustainable technologies that can be implemented in resource-limited areas [4,5].

Biosand filtration (BSF) is a well-established point-of-use (POU) water treatment method that leverages natural filtration processes to remove suspended solids, heavy metals, and microbial contaminants [6-8]. Originally developed as an adaptation of slow sand filtration, BSF consists of a simple design incorporating layers of sand and gravel, with a biologically active layer (schmutzdecke) that enhances microbial reduction [9,10]. The system operates through a combination of mechanical trapping, adsorption, predation, and natural die-off of pathogens [11,12]. Despite its proven effectiveness, conventional BSF units may have limitations in removing certain chemical pollutants and achieving consistent physical and microbial disinfections under varying environmental conditions [13,14].

Numerous studies have explored the effectiveness of BSF and natural materials in improving water quality, focusing on physicochemical and microbial contaminant removal. Abdiyev et al. [15] investigated the synergistic effects of natural adsorbents in BSFs, incorporating sand with organic media

such as coconut shells and papyrus fibers. They used a long-term field study approach and found that microbial removal was consistent at 99%, with significant improvements in reducing nitrates and phosphates. Mulugeta et al. [16] conducted an experimental study using modified BSFS with activated carbon and natural coagulants to enhance microbial removal. Their findings demonstrated that incorporating biochar significantly improved the reduction of E. coli and total coliforms, achieving an efficiency of over 98%. Emslie et al. [17] applied mathematical modeling to optimize BSF design for rural water treatment. Their numerical simulations validated that flow rate adjustments and biofilm development stages influence filter performance, leading to improved removal of coliform bacteria and suspended solids. Dandadzi et al. [18] carried out a comparative analysis of BSF with and without organic media amendments, focusing on field applications in developing regions. They reported that filters supplemented with organic fibers exhibited 20% higher contaminant removal efficiency than traditional sand-based filters. Ganesan et al. [19] examined the use of cane papyrus fibers as a bioadsorbent in BSF. Their study employed batch and column experiments, revealing that cane papyrus improved turbidity reduction by 75% and enhanced the removal of dissolved organic carbon by 65%, making it a promising natural enhancement material. Sharma et al. [20] explored the performance of biofilm-enhanced BSFs for removing heavy metals from water. Using controlled laboratory conditions, they reported that the presence of biofilm layers facilitated increased adsorption rates of lead (Pb) and arsenic (As), with removal efficiencies reaching 92% and 89%, respectively. Mahmood et al. [21] developed a hybrid BSF with antimicrobial coatings and conducted pilot-scale testing in various environmental conditions. Their study found that the filters maintained stable pathogen removal efficiency of 99.5% over six months, demonstrating resilience to fluctuating water quality parameters. Tsafack et al. [22] investigated BSF modifications using silver-impregnated media for enhanced pathogen reduction. Through controlled laboratory trials, they confirmed that the modified filters achieved a 3-log reduction in viruses and protozoa, significantly outperforming conventional BSFs. Recent studies in 2025 have emphasized sustainable approaches to BSF [23,24]. Ongoing research explores the integration of advanced nanomaterials and machine learning-based predictive models to optimize performance [25,26]. Overall, advancements in BSF research have highlighted the critical role of natural enhancements, microbial biofilms, and predictive modeling in achieving higher efficiency in water treatment. These studies collectively provide a strong foundation for further optimizing BSF designs using sustainable and cost-effective materials.

To improve the efficiency of BSF, recent research has explored the integration of natural adsorbents and bioactive materials. Organic fibers such as Cane Papyrus, which are abundant in wetland ecosystems, have been identified as promising natural materials for enhancing contaminant removal. The fibrous structure of Cane Papyrus provides increased surface area for adsorption, supports biofilm growth, and facilitates the removal of organic and inorganic pollutants. The use of such materials aligns with sustainable water treatment approaches, promoting the utilization of locally available resources to improve filtration performance.

This study aims to investigate the effectiveness of an enhanced BSF system incorporating Cane Papyrus fibers in removing physicochemical and microbial contaminants from water. To determine the extent of contaminant removal under enhanced BSF, key water quality parameters, including temperature, pH, turbidity, total dissolved solids (TDS), Electrical conductivity (EC), total hardness (TH), calcium (Ca^{2+}), magnesium (Mg^{2+}), chloride (Cl^{-}), sulfate (SO_4^{2-}), and Escherichia coli (E. coli), were analysed. Additionally, the study employs statistical analysis, to assess variations in removal efficiency across different filtration configurations. Reduction efficiency calculations were also performed to quantify the removal performance of each setup. It is hypothesized that the addition of Cane Papyrus to the BSF enhances filtration efficiency by increasing adsorption capacity and promoting biofilm activity. The results of this study are expected to provide valuable insights into the feasibility of integrating organic fiber-based enhancements in BSF systems, contributing to the development of cost-effective and scalable solutions for improving drinking water quality in underserved communities.

2. Materials and Methods

2.1 Study Area Description

The study was conducted in Al-Hindiya District, Karbala Governorate, Iraq, located at approximately 32.5° N latitude and 44.2° E longitude (see Fig. 1). Al-Hindiya is a crucial agricultural and industrial hub, with water bodies exposed to pollutants from various sources, including industrial effluents, agricultural runoff, and residential wastewater discharge. The district relies heavily on surface water resources, particularly the river and its branches climate change, which serve as primary sources

for drinking and irrigation [27]. The river serves as the primary water source for the area, exhibiting seasonal fluctuations in flow rate and carrying high sediment loads.

However, rapid urbanization and increased human activities have contributed to a decline in water quality, necessitating the development of effective filtration techniques to ensure safe drinking water. Water in Al-Hindiya is often unsuitable for direct consumption due to elevated concentrations of dissolved solids, heavy metals, microbial contaminants (e.g., E. coli), and suspended particles. The study area represents a critical zone for water treatment research, as improving water quality directly impacts public health and agricultural sustainability. Al-Hindiya region was chosen for samples collected during experimental study, due to the high level of water contamination, making it an ideal location for evaluating the effectiveness of a BSF modified with Cane Papyrus as an adsorbent.

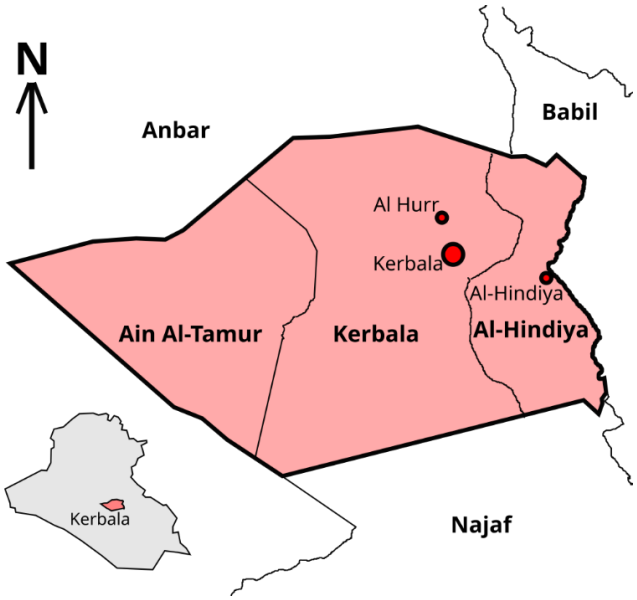

Fig. 1: Al-Hindiya District location.

2.2 Sample Collecting

Sixty Water samples were collected from multiple locations within Al-Hindiya District to ensure a representative dataset of contamination levels across different sources. Local water bodies that are contaminated by different sources such as industrial effluent zones, where factories and workshops discharge untreated water, agricultural runoff points, where chemical fertilizers and pesticides contribute to elevated nitrate and phosphate levels, and residential wastewater discharges, where untreated sewage and domestic waste enter local water bodies.

To assess pre-treatment water quality, samples were collected before reaching the water treatment stations. Glass and polyethylene bottles were used for collection, pre-cleaned with deionized water, and sterilized to prevent contamination. All glass and polyethylene bottles were sterilized by autoclaving at 121°C for 15 minutes and that single-use disposable bottles were also employed where applicable. Each sample was carefully labelled with date, time, temperature, and source details to ensure sample integrity. Sample collections were followed according to APHA (Standard Methods for the Examination of Water and Wastewater, 23rd edition) to ensure the quality and reliability of the samples. Samples were stored in coolers at 4°C and transported to the laboratory within 6 hours to minimize biological and chemical changes.

Strict quality control measures were implemented throughout the process. Field blanks and duplicates were included to verify data accuracy, while pH and temperature were measured on-site to prevent alterations during transportation. Additionally, sterile gloves and sampling kits were used to eliminate external contamination, ensuring reliable and precise results.

2.3 Contaminant Assessment

Water samples were analyzed for physical, chemical, and microbial contaminants to determine the efficacy of the BSF under controlled conditions. Each contaminant was selected based on its impact on water quality, health risks, and relevance to BSF performance. pH and temperature influence chemical reactions and microbial activity in water, while turbidity serves as an indicator of suspended particles

that may harbor pathogens. EC and TDS represent the concentration of dissolved ions, affecting water salinity. TH, Ca^{+2}, and Mg^{+2} impact water hardness, influencing taste, scaling, and corrosion. Cl^{-1} and SO_4^{2-} at high levels contribute to salinity and may have corrosive effects on infrastructure. E. coli serves as a key indicator of fecal contamination and potential pathogens in water.

3 Experimental Setups and Scenarios

3.1 BSF Design

The BSF was designed and constructed to assess its effectiveness in removing contaminants from collected water samples. To enhance its filtration efficiency, the filter was modified with Cane Papyrus (Cyperus papyrus) as an adsorbent material.

The BSF was built using a cylindrical plastic container with a total height of 48 cm and an internal diameter of 26 cm, as presented in Fig. 2. The filter consists of several key layers, each playing a crucial role in the filtration process. Inside the container, the filtration media were arranged in a specific sequence of layers: a 20 cm layer of fine sand (with a particle size of 1 mm), a 5 cm layer of coarse sand (with a particle size of 6 mm), and a 5 cm layer of gravel (with a particle size of 15 mm). The inlet chamber allows raw water to enter gradually, preventing turbulence. A diffuser glass plate, a perforated sustainable structure, ensures even distribution of the inflow [28-31]. At the heart of the filtration process is the biological layer (Schmutzdecke), a microbial biofilm that actively degrades organic contaminants. Beneath this, the fine sand layer acts as the primary filtration medium, removing suspended solids and microbial contaminants through mechanical straining and adsorption. The sand used in the filter had an effective diameter (D_{10}) and a uniformity coefficient (Cu) of 2.5, indicating a well-graded material suitable for slow sand filtration. The sand was thoroughly washed and sieved to achieve the desired specifications, ensuring optimal removal efficiency and minimizing clogging risk. The coarse sand layer provides additional filtration while preventing clogging. A gravel layer at the bottom serves as a supporting medium, ensuring structural stability and facilitating proper drainage. Finally, an outlet pipe maintains a constant water level and allows the filtered water to exit the system. It is worth noting that the discharge from the plastic container was measured using a flow meter, which was systematically placed at the end of the container.

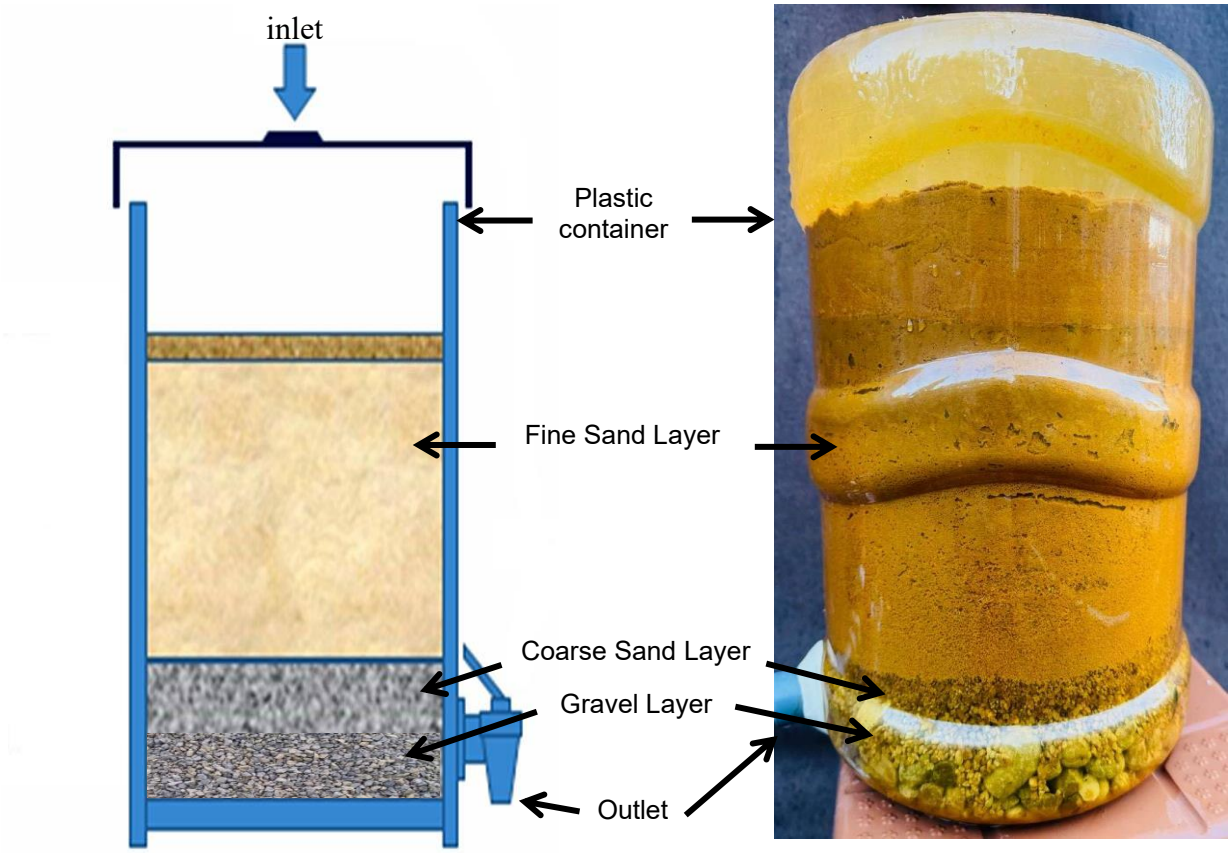

Fig. 2: BSF design and layer configuration.

The BSF was constructed using multiple layers, each serving a specific function in the filtration process. The biological layer, with a thickness of 1-5 cm, facilitates microbial degradation of organic contaminants. Below this, a 20 cm fine sand layer with a grain size of 1 mm provides particle filtration, effectively removing suspended solids and pathogens. A 5 cm coarse sand layer, with a grain size of 6 mm, offers additional filtration, preventing clogging and improving water flow. At the base, a 5 cm gravel layer with a grain size of 15 mm ensures structural support and proper drainage.

To enhance the adsorption capacity of the filter, Cane Papyrus fibers were incorporated into the fine sand layer. The preparation of the adsorbent material involved several steps. First, the papyrus was dried and cut into 2-5 mm pieces. It was then pre-washed with distilled water to remove impurities that could interfere with adsorption. Finally, the material underwent heat activation at 105°C for 4 hours, a process that increases its surface area and enhances its ability to capture contaminants.

A biological layer (Schmutzdecke) was developed to enhance microbial degradation of organic contaminants in the BSF system [12]. This layer consists of naturally occurring bacteria and microorganisms that attach to the fine sand layer and feed on organic matter in the water, significantly improving the filtration process. To establish the biofilm, a mixture of river water and previously matured filter media was introduced to seed beneficial bacteria. The filter was then kept moist for 15-20 days to allow biofilm growth, with periodic additions of a low-concentration glucose solution to provide essential nutrients for microbial colonization [12]. The biofilm's maturation was monitored through visual inspection, including changes in color, bio-layer thickness, and the presence of gas bubbles on the sand surface, as shown in Fig. (3). Additionally, total coliform and heterotrophic plate counts were performed to verify microbial activity. The sand was incubated in a controlled environment for 14 days, with temperature, humidity, and nutrient availability carefully regulated to promote biofilm development. Once fully established, the biofilm played a crucial role in breaking down organic pollutants and reducing pathogen levels, contributing to the overall effectiveness of the filtration system.

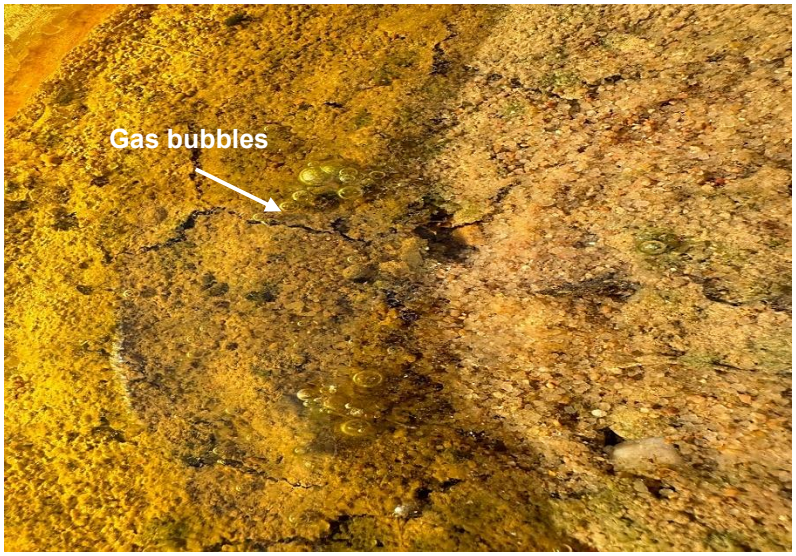

Fig. 3: Visible biofilm formation on sand after 14 days of incubation.

The model integrates hydraulic flow, adsorption kinetics, and microbial biofilm activity to assess contaminant removal efficiency. The BSF was conceptualized using a layered filtration model, considering several key parameters:

Hydraulic retention time: Evaluates the water residence time within the filter.

Filtration rate: Determined using Darcy's Law, which governs the flow of water through porous media.

Contaminant removal kinetics: Predicts pathogen and pollutant reduction over time [32]. Mathematically, the filtration model is represented as:

$$Q = KA\left(\frac{\Delta H}{L}\right) \quad (1)$$

where Q: Filtration rate (m³/s); K: Hydraulic conductivity (m/s); A: Cross-sectional area of the filter (m²) ΔH: Hydraulic head difference (m); and L: Depth of filtration media (m).

A contaminant adsorption model was designed using papyrus reed (Cyperus papyrus) as an adsorbent to enhance contaminant removal [33]. The initial water content has a significant impact on

the collapsibility of natural soils, especially those exposed to water currents and waves, which in themselves simulate the biological activity of soils and other materials internal to any structure design [34,35]. The biological activity within the filter was simulated using first-order microbial degradation kinetics, represented by:

$$C_t = C_0 e^{-kt} \quad (2)$$

where C_t: Contaminant concentration at time; C_0: Initial contaminant concentration; k: Reaction rate constant (dependent on microbial activity); and t: Contact time in the filter.

This model provides a comprehensive framework for evaluating BSF performance and optimizing design parameters to enhance water treatment efficiency.

3.2 Measured Properties and Methods of Measurement

To evaluate the performance of the BSF, several key physicochemical and microbial water quality parameters were measured. The contaminants assessed in this study and their measurement methods are summarized in Table 1.

Table 1. Measured parameters properties.

Parameter	Unit	Measurement Equipment	Manufacturer and Model
pH	-	Digital pH Meter	Hanna Instruments, HI98103
Temp.	[°C]	Laboratory Thermometer	Hanna Instruments, HI98509
Turb.	[NTU]	Turbidity Meter	Hach, 2100Q
EC	[µS/cm]	Conductivity Meter	Hach, HQ40d
TDS	[mg/L]	Water Quality Meter	Hach, HQ40d
TH	[mg/L]	Burette and Indicator (Titration Method)	Manual (standard method, ASTM D1126)
Ca^{2+}	[mg/L]	Titration Equipment (EDTA method)	INB400 (local manufacture)
Mg^{2+}	[mg/L]	Titration Equipment (EDTA method)	INB400 (local manufacture)
Cl^-	[mg/L]	Titration Equipment (Silver Nitrate method)	Metrohm, 848 Titrino Plus
SO_4^{2-}	[mg/L]	UV-Visible Spectrophotometer	Shimadzu, UV-1800
E. coli	[CFU/mL]	Membrane Filtration + Incubator	Millipore Filtration System + Memmert Incubator

3.3 Filter Operation and Scenarios

The filter was operated intermittently for two hours every 48 hours, to prevent clogging and ensure consistent performance. During each test, the contaminated water was poured into the container, ensuring a water height of 5-7 cm above the diffuser plate. After each run, samples were collected from the filter outlet and analyzed for physical, chemical, and microbial properties. The experimental design considered various operational parameters, as outlined in Table 2.

Table 2. Operational parameters and testing conditions for the enhanced BSF.

Scenario	Variable	Value Tested	Justification
Biological Layer [BL]	Thickness	1, 2, 5 (cm)	Assessing biofilm development and effectiveness
[pH	pH Levels	4.01, 6.86, 9.18	Evaluating filtration performance under varying acidity/alkalinity
Temperature	Temperature	5, 25, 35 (°C)	Studying the effect of temperature on microbial activity and contaminant removal
Flow Rate [Q]	Flow Rate	0.5, 2, 5 (m/h)	Determining the optimal filtration rate for contaminant removal
Time [T]	Exposure Time	12, 24, 36, 48 (min)	Evaluating the impact of retention time on treatment efficiency

The filtration process began with water addition, where contaminated water was poured into the inlet chamber. To ensure even distribution and prevent disturbance of the biofilm, a diffuser plate regulated the water flow. During physical filtration, suspended solids were trapped in the fine sand layer, while larger particles were removed in the coarse sand and gravel layers. Following this, biological degradation occurred in the biofilm layer, where microbial activity decomposed organic contaminants and pathogens. Finally, water collection took place as the treated water exited through the outlet pipe, where it was analyzed for quality improvements. To comprehensively evaluate BSF performance, water samples were analyzed under baseline conditions, comparing contaminant levels before and after filtration. The study considered key influencing factors such as pH, temperature, flow rate, biological layer thickness, and retention time to determine their impact on filtration efficiency. The removal efficiency of each contaminant was calculated using the formula:

$$Removal\ Efficiency(\%) = \left(\frac{Initial\ Concentration - Final\ Concentration}{Initial\ Concentration}\right) \times 100 \quad (3)$$

Statistical analysis was applied to determine the significance of parameter variations of the data collected in this study.

4 Results and Discussion

This study evaluated the performance of the bio-sand filter (BSF) under varying operational conditions, including biological layer thickness, pH, temperature, flow rate, exposure time, and adsorption enhancement (as illustrated in Fig. 4a-k). The findings highlight the influence of these parameters, polluted model (PM), temperatures of 5°C (Temp. 1), 25°C (Temp. 2), and 35°C (Temp. 3), biological layer thicknesses of 1 mm (BL1), 2 mm (BL2), and 5 mm (BL3), pH values of 4.01 (pH1), 6.86 (pH2), and 9.18 (pH3), exposure times of 12 hours (T1), 24 hours (T2), and 48 hours (T3), and flow rates of 0.5 m/h (Q1), 2 m/h (Q2), and 5 m/h (Q3) on contaminant removal efficiency.

4.1 pH variations

The pH values in the biosand filter system were influenced by various factors, including biological layer thickness, temperature, and environmental conditions, which impacted the overall water treatment efficiency. Figure 4a presents the pH values under different conditions, showing the initial pH of the polluted model (PM) at 7.12, which is slightly lower than the values observed with biological layers. As the biological layer thickness increases, the pH rises, reaching 7.6 for BL1 and stabilizing at 7.8 for BL2 and BL3. This suggests that the biological layer has a neutralizing effect, possibly due to microbial activity or buffering capacity, and the pH stabilizes at a certain layer thickness, indicating equilibrium. Figure 4b presents pH variations under different conditions. The initial pH of the PM is 7.12, and the recorded pH values for different conditions (pH1, pH2, and pH3) show significant fluctuations. pH1 measures 4, indicating a highly acidic environment, potentially due to industrial discharge or acidification. pH2 at 6.9 is closer to neutral but still slightly acidic, while pH3 at 9.3 shows an alkaline condition, which could result from the presence of alkaline compounds or treatment interventions. These variations highlight the dynamic nature of water chemistry and its susceptibility to external factors.

Figure 4c shows pH variations under different temperature conditions. The initial PM pH is 7.12, and as the temperature changes, the pH fluctuates. At Temp. 1, the pH decreases to 6.3, indicating acidity, possibly due to increased CO_2 solubility in colder conditions. Temp. 2 has a pH of 6.9, closer to neutrality, and Temp. 3 shows a pH of 7.7, indicating alkalinity. These changes emphasize the effect of temperature on water chemistry, affecting gas dissolution and buffering capacity. Figure 4d displays pH variations of the PM under different conditions labeled Q1, Q2, and Q3. The initial pH of 7.12 decreases slightly to 7.0 in Q1, increases to 7.4 in Q2, and then returns to 7.1 in Q3. These variations suggest that factors like chemical reactions, biological activities, and environmental conditions influence pH. Figure 4e presents pH values of the PM under three conditions labeled T1, T2, and T3. The initial pH of 7.12 increases to 7.5 in T1, further rises to 7.8 in T2, and then decreases to 7.1 in T3. These variations reflect the influence of environmental factors on pH and water quality stability.

In conclusion, biological layer thickness and temperature had the most significant effects on pH stabilization and the overall efficiency of the biosand filter system. Thicker biological layers and higher temperatures contributed to better pH stabilization and enhanced water treatment performance. Flow rate and exposure time also played a role but were less impactful compared to biological layer thickness and temperature. Therefore, optimizing these two factors should be prioritized to achieve maximum treatment efficiency and improved water quality management.

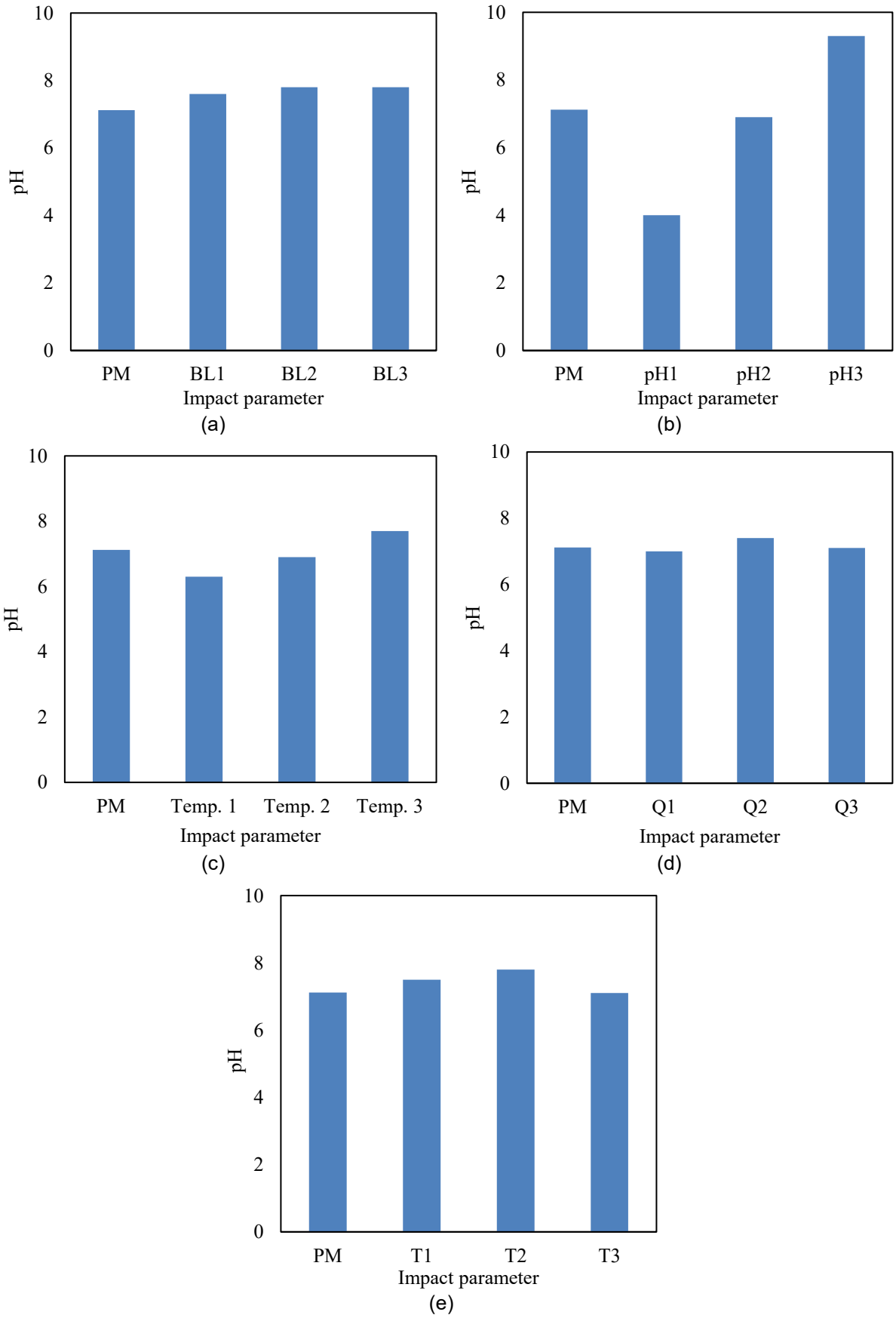

Fig. 4: Water quality parameters results under pH variation of the enhanced BSF.

4.2 Turbidity variations

The turbidity removal in the biosand filter system was significantly influenced by various parameters, including biological layer thickness, pH, temperature, flow rate, and exposure time.

The best turbidity removal occurred at a 2 mm biological layer thickness, where turbidity dropped to 4 NTU, indicating optimal filtration. At 1 mm, turbidity was 7 NTU, and at 5 mm, it increased to 5.6 NTU, suggesting that a thicker layer could reduce efficiency due to increased resistance and clogging. Figure 5a illustrates turbidity values across different biological layer thicknesses.

Neutral pH showed the best turbidity removal, with a turbidity of 3 NTU. Acidic and alkaline conditions led to higher turbidity values of 10 NTU and 9 NTU, respectively, indicating that extreme pH levels reduce filtration efficiency. Figure 5b shows turbidity under different pH conditions.

The optimal temperature for turbidity removal was 25°C, where turbidity was 5 NTU. Both lower temperatures (5°C) and higher temperatures (35°C) showed slightly higher turbidity, indicating that moderate temperatures support the best microbial activity for filtration. Figure 5c depicts turbidity values at different temperatures.

A higher flow rate resulted in the lowest turbidity value of 2 NTU, indicating that faster filtration is more efficient. Slower flow rates, such as 0.5 m/h, resulted in higher turbidity due to insufficient interaction time with the filter. Figure 5d displays turbidity values for different flow rates.

The longest exposure time of 48 hours achieved the best turbidity removal at 3.4 NTU. Shorter exposure times, such as 12 hours, resulted in higher turbidity, indicating that more time for microbial and physical processes enhances filtration efficiency. Figure 5e shows turbidity at different exposure times.

In summary, the optimal conditions for turbidity removal were found to be a 2 mm biological layer thickness, neutral pH, moderate temperature (25°C), higher flow rate (5 m/h), and longer exposure time (48 hours), with each factor working synergistically to enhance filtration efficiency. Understanding and optimizing these parameters is essential for designing effective water treatment systems.

4.3 Temperature variations

The turbidity values presented in Figure 6a show how biological layer thickness and temperature impact filtration efficiency. The turbidity values for BL1 (1 mm) at 27°C were 7 NTU, while BL2 (2 mm) exhibited the lowest turbidity at 25°C with 4 NTU. BL3 (5 mm) had a turbidity of 5.6 NTU at 26°C, indicating that an increase in layer thickness slightly reduces filtration efficiency. However, the temperature did not significantly affect turbidity, with the best performance observed at 25°C, suggesting that microbial activity is optimal at this temperature for particle removal.

The turbidity also varied with pH levels, as shown in Figure 6b. At 25°C, turbidity was lowest at neutral pH (pH2) with 3 NTU, indicating efficient contaminant removal. At acidic pH (4.01) and alkaline pH (9.18), turbidity increased to 10 NTU and 9 NTU, respectively. These higher turbidity levels suggest that extreme pH values impair microbial activity and alter the solubility of contaminants, reducing filtration efficiency.

Figure 6c illustrates turbidity variations under different temperature conditions. The lowest turbidity (5 NTU) occurred at 25°C, indicating optimal filtration efficiency with high microbial activity. At 7°C (Temp. 1), turbidity increased to 5.1 NTU, suggesting reduced microbial activity at lower temperatures. At 36°C (Temp. 3), turbidity was 4.9 NTU, indicating that higher temperatures could increase the dissolution of contaminants, affecting microbial degradation and filtration performance.

Flow rate also impacted turbidity removal, as presented in Figure 6d. At higher flow rates, turbidity removal improved, with Q3 (5 m/h) achieving the best performance at 2 NTU, suggesting that faster flow rates enhance filtration efficiency. At slower flow rates, such as Q1 (0.5 m/h), turbidity was higher (12 NTU), indicating poor filtration due to reduced contact time, despite the optimal temperature of 26°C.

Exposure time played a critical role in turbidity removal, as shown in Figure 6f. The longest exposure time (T3, 48 hours) resulted in the lowest turbidity (3.4 NTU), suggesting that extended exposure allows for better microbial growth and contaminant degradation. In contrast, shorter exposure times (T1, 12 hours) led to higher turbidity (5 NTU), indicating that insufficient time hinders effective filtration.

In conclusion, temperature significantly affects turbidity removal in biosand filtration systems, with moderate temperatures (around 25-26°C) offering optimal conditions for microbial activity and filtration performance. Extremes of temperature (either too low or too high) impair microbial activity and promote the dissolution of contaminants, increasing turbidity. Additionally, exposure time, flow rate, and biological layer thickness also influence filtration efficiency, with longer exposure times and higher flow rates further improving turbidity removal, especially when combined with optimal temperature conditions.

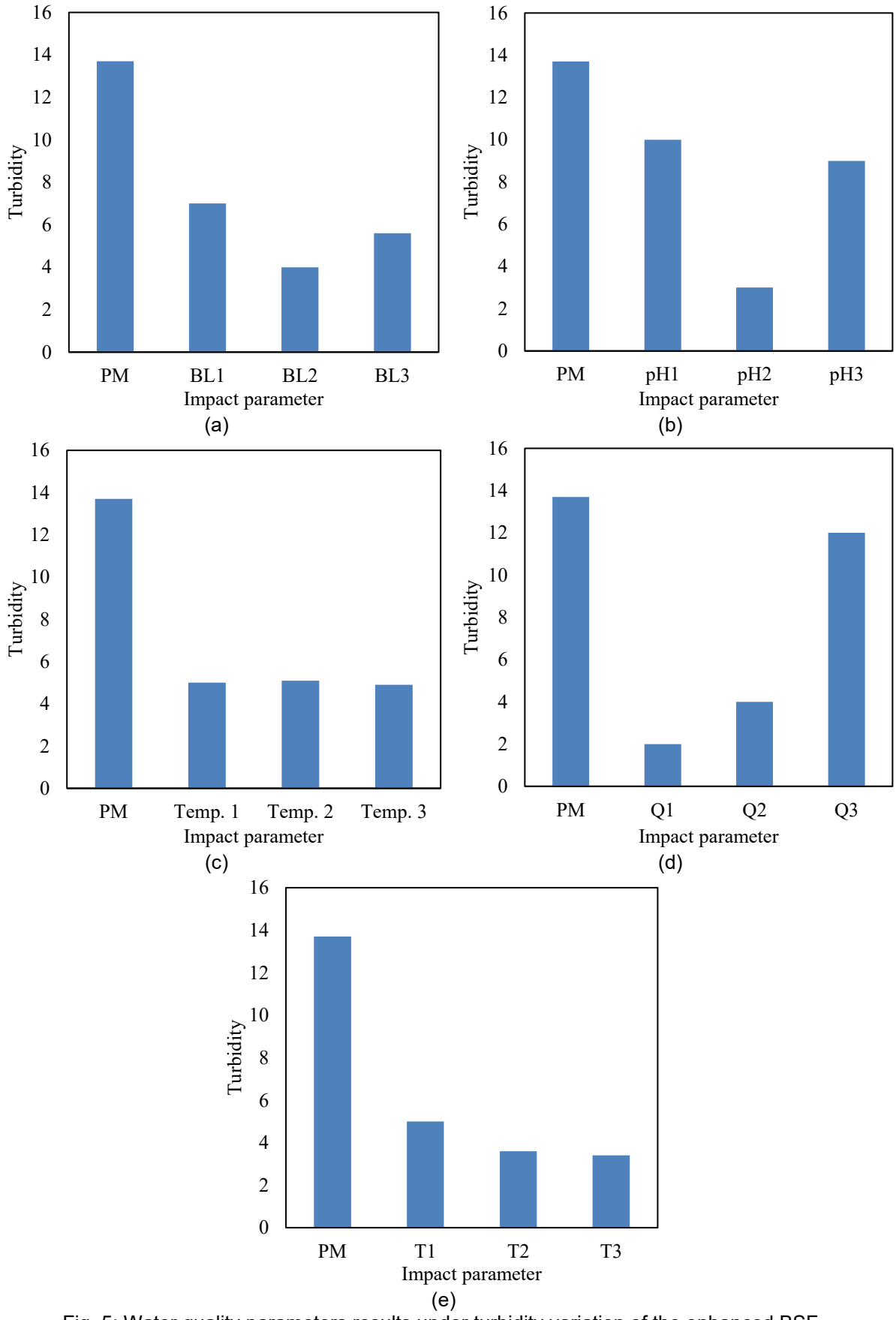

Fig. 5: Water quality parameters results under turbidity variation of the enhanced BSF.

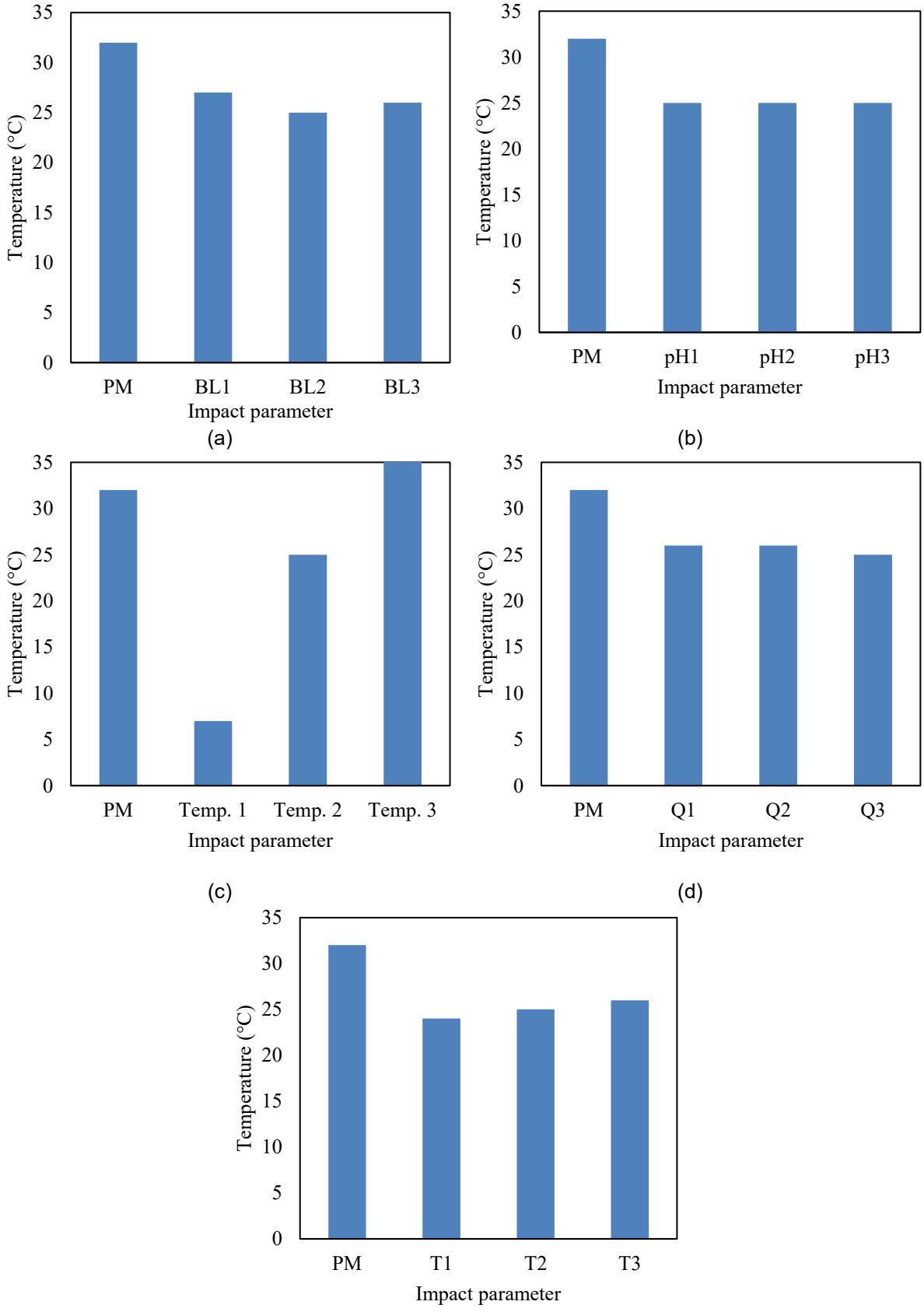

Fig. 6: Water quality parameters results under temperature variation of the enhanced BSF.

4.4 EC variations

The Electrical Conductivity (EC) values, as shown in Figure 7a, demonstrate the impact of biological layer thickness on ion removal in biosand filtration systems. The EC in the Polluted Model (PM) is high at 2710 µS/cm, indicating a high concentration of dissolved ions and contaminants. As the biological layer thickness increases, EC values decrease: BL1 (1 mm) shows 1466 µS/cm, BL2 (2 mm) shows 1255 µS/cm, and BL3 (5 mm) shows 1360 µS/cm. The decrease in EC with increasing biological layer thickness suggests that the filter's ability to remove dissolved ions improves as the layer thickens. In BL1, the relatively high EC could be due to insufficient microbial interaction or limited ion adsorption, while in BL2, the thicker layer seems to enhance filtration efficiency and reduce EC.

As illustrated in Figure 7b, EC values also decrease under varying pH conditions. The lowest EC occurs at neutral pH (pH2, 6.86), which indicates effective ion removal by the biosand filter, with an EC of 1067 µS/cm. In contrast, at acidic (pH1, 4.01) and alkaline (pH3, 9.18) conditions, EC increases to 1167 µS/cm and 1222 µS/cm, respectively. The higher EC at extreme pH levels suggests that pH influences the solubility and ionization of contaminants, which in turn affects the filter's ability to remove dissolved ions. Neutral pH likely provides the most favorable environment for filtration, facilitating effective ion removal and reducing EC.

In Figure 7c, the EC values under varying temperature conditions show a clear trend. At Temp. 1 (7°C), EC is 1212 µS/cm, while at Temp. 2 (25°C), it reaches the lowest value of 1084 µS/cm, indicating optimal conditions for ion removal. At Temp. 3 (36°C), the EC increases to 1800 µS/cm, suggesting that higher temperatures enhance the solubility of salts and other ions, leading to higher EC values. This pattern highlights that temperature significantly influences ion solubility and dissolution, with moderate temperatures promoting more effective ion removal. Figure 7d demonstrates the influence of flow rate on EC values. As flow rate increases, EC also increases, with Q1 (0.5 m/h) yielding 1190.5 µS/cm, Q2 (2 m/h) showing 1097 µS/cm, and Q3 (5 m/h) having the highest EC of 1545 µS/cm. Faster flow rates reduce contact time between water and the biological layer, which may decrease ion removal efficiency, leading to higher EC values. The results suggest that slower flow rates, which allow for longer contact time, are more effective in reducing EC by allowing more time for ion adsorption and removal.

In Figure 7e, the relationship between exposure time and EC values shows a trend of decreasing EC with longer exposure times. At T1 (12 hours), EC is 1124 µS/cm, slightly lower than the initial EC in the PM. At T2 (24 hours), EC decreases further to 1130 µS/cm, and at T3 (48 hours), it reaches the lowest value of 1080 µS/cm. Longer exposure times provide more opportunities for microbial activity and ion adsorption, leading to more effective ion removal and a reduction in EC. This suggests that extended exposure is beneficial for achieving the lowest EC values.

4.5 TDS variations

The data on Total Dissolved Solids (TDS) demonstrates the significant impact of biological layer thickness, pH, temperature, flow rate, and exposure time on water quality in biosand filtration systems.

Biological Layer Thickness (Figure 8a): TDS decreases with increasing biological layer thickness, with the Polluted Model (PM) showing a high TDS of 1761.5 mg/L. As the biological layer thickness increases, TDS values reduce: BL1 (1 mm) shows 744 mg/L, BL2 (2 mm) shows 668.83 mg/L, and BL3 (5 mm) shows 712 mg/L. The initial biological layers (BL1 and BL2) are most effective at reducing TDS, with diminishing returns as the layer becomes thicker.

pH Conditions (Figure 8b): TDS values show variation under different pH levels. The lowest TDS value occurs at pH1 (acidic, 4.01), where TDS is 609 mg/L, suggesting enhanced precipitation of ions or compounds. At neutral pH (pH2, 6.86), TDS slightly increases to 616.53 mg/L, while at alkaline pH (pH3, 9.18), TDS increases further to 740 mg/L due to the dissolution of certain minerals and salts at higher pH levels. Temperature (Figure 8c): TDS values fluctuate with temperature. At lower temperatures (7°C), TDS is the highest at 800.12 mg/L, while at moderate temperature (25°C), TDS decreases to 680.75 mg/L, and at higher temperature (36°C), TDS rises again to 740 mg/L. The solubility of salts and minerals plays a crucial role in TDS concentration, with the moderate temperature offering optimal conditions for TDS reduction. Flow Rate (Figure 8d): TDS increases with increasing flow rate. At the lowest flow rate (0.5 m/h), TDS is 633.59 mg/L, and as the flow rate increases to 2 m/h and 5 m/h, TDS rises to 650 mg/L and 1098 mg/L, respectively. The higher flow rates result in reduced contact time between water and the biological filter, leading to less effective filtration and a higher concentration of dissolved solids.

Exposure Time (Figure 8e): TDS slightly decreases with longer exposure times. At 12 hours (T1), TDS is 712 mg/L, and at 48 hours (T3), it drops to 687 mg/L. The reduction in TDS over extended

exposure times suggests that prolonged filtration improves the removal of dissolved solids through processes such as adsorption and precipitation.

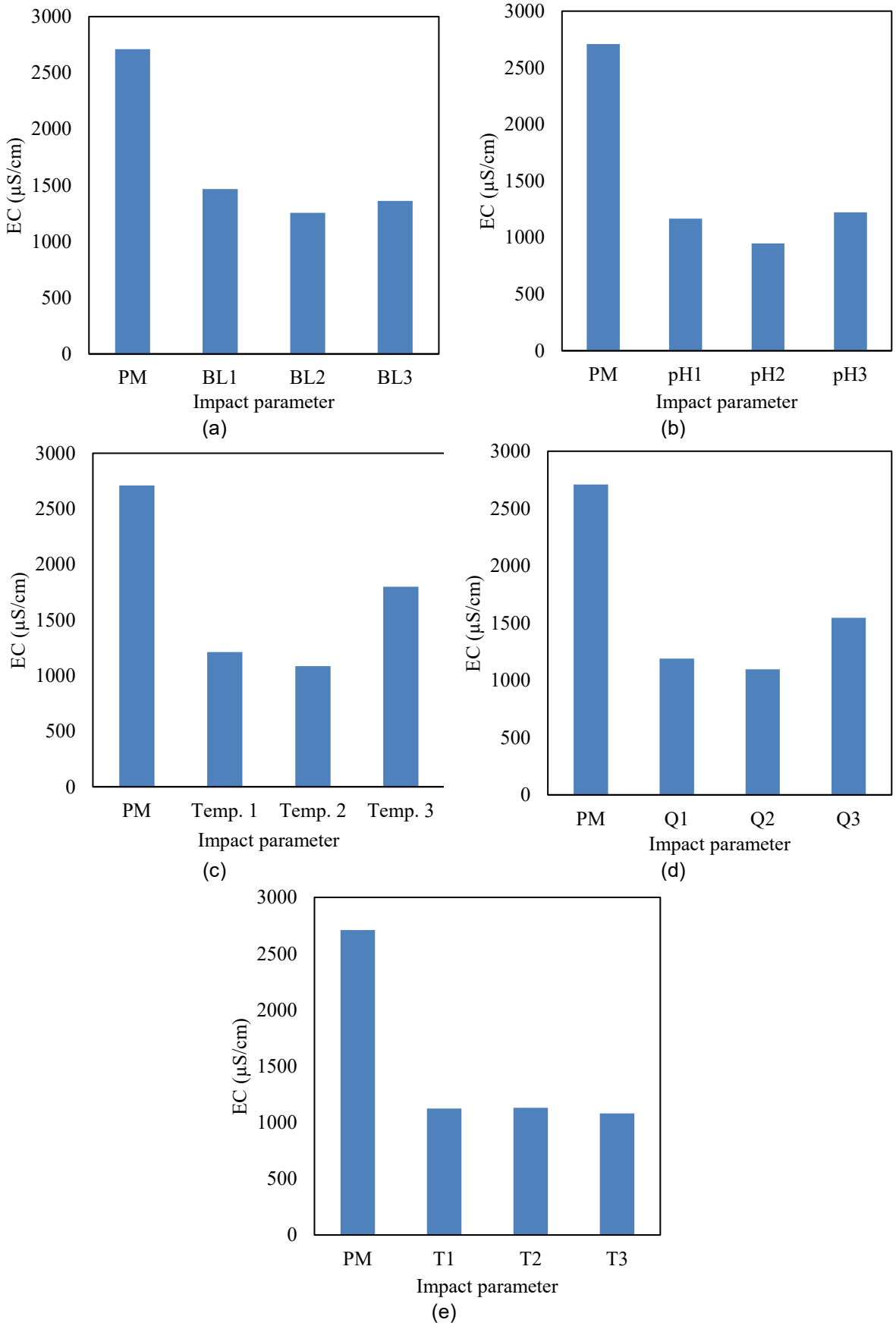

Fig. 7: Water quality parameters results under temperature variation of the enhanced BSF.

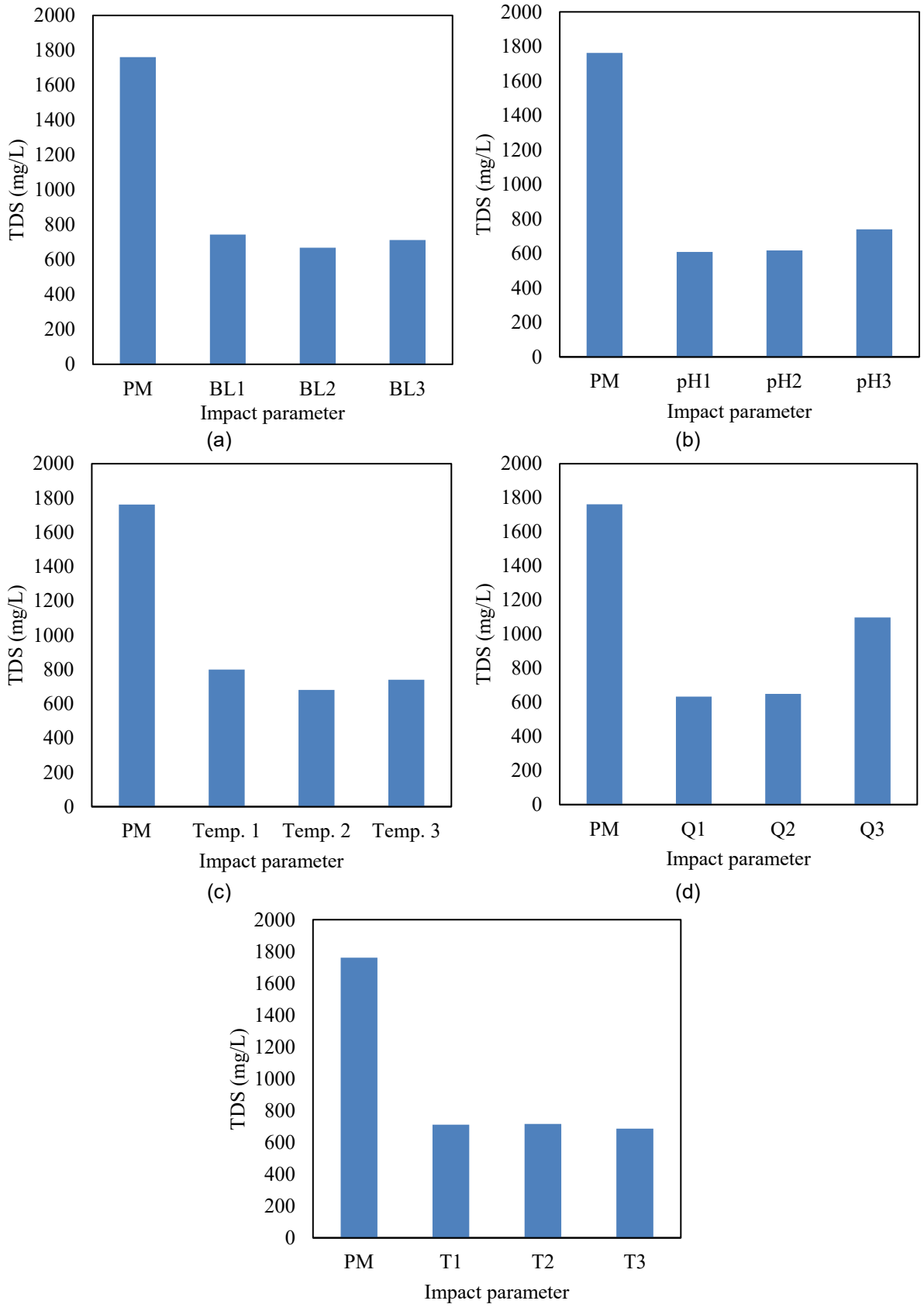

Fig. 8: Water quality parameters results under TDS variation of the enhanced BSF.

4.6 TH variations

Total Hardness (TH) decreases significantly with increasing biological layer thickness, as shown in Figure 9(a). Initially, at PM (Polluted Model), TH is 1120 mg/L, indicating high hardness. As the biological layer thickness increases, TH decreases: BL1 (1 mm) shows 723 mg/L, BL2 (2 mm) shows 625 mg/L, and BL3 (5 mm) shows 819 mg/L. This suggests that biological filters are most effective at removing hardness with thinner layers (BL1 and BL2), but the effectiveness reduces at greater thicknesses (BL3), likely due to reduced interaction time between the water and the filter material.

TH values also change with varying pH conditions, as shown in Figure 9(b). At acidic pH1 (4.01), TH is 796 mg/L, slightly reduced from the initial PM value. At neutral pH2 (6.86), TH decreases further to 593 mg/L. At alkaline pH3 (9.18), TH rises to 918.4 mg/L. The reduction at neutral pH suggests that hardness-causing ions such as calcium and magnesium are precipitating or binding with other substances, making them less soluble. In contrast, the increase at alkaline pH may be due to the enhanced solubility of certain salts, which dissolves hardness-causing minerals.

Temperature fluctuations also affect TH, as seen in Figure 9(c). At a lower temperature (7°C), TH is 623.8 mg/L, the lowest among the three temperatures. At a moderate temperature (25°C), TH increases to 523 mg/L, and at a higher temperature (36°C), TH reaches 860 mg/L. The decrease at moderate temperatures may be due to increased precipitation or enhanced ion exchange, whereas the higher temperature may increase the solubility of hardness-causing minerals, leading to higher TH levels.

Flow rate influences TH as well, as illustrated in Figure 9(d). At a flow rate of Q1 (0.5 m/h), TH is 493 mg/L, the lowest among the three flow rates. At Q2 (2 m/h), TH increases to 580 mg/L, and at Q3 (5 m/h), TH further increases to 995 mg/L. The increase at higher flow rates is due to reduced contact time between the water and biological material, which diminishes the filter's ability to remove hardness-causing ions. This indicates that slower flow rates improve filtration efficiency and reduce hardness levels.

TH values also show a reduction over longer exposure times, as shown in Figure 9(e). At 12 hours (T1), TH is 857 mg/L, the highest. At 24 hours (T2), TH decreases to 719 mg/L, and at 48 hours (T3), it drops further to 512 mg/L. The reduction over time suggests that longer exposure enhances the filter's ability to remove hardness-causing ions through ion exchange or precipitation.

4.7 Ca variations

The calcium concentration (Ca) shows a significant decrease with increasing biological layer thickness, as illustrated in Figure 10(a). At PM (Polluted Model), calcium is 256 mg/L. As the biological layer thickness increases, the calcium concentration decreases: BL1 (1 mm) has 183 mg/L, BL2 (2 mm) has 153 mg/L, and BL3 (5 mm) has 167 mg/L. This suggests that the biological filter is most effective at removing calcium in thinner layers (BL1 and BL2), but the efficiency reduces at BL3, possibly due to reduced interaction time between the water and filter media as the layer thickness increases.

Calcium concentration also varies with pH levels, as shown in Figure 10(b). At acidic pH1 (4.01), calcium decreases to 98 mg/L. At neutral pH2 (6.86), it increases to 89.6 mg/L, and at alkaline pH3 (9.18), it rises to 109 mg/L. In acidic conditions, calcium ions tend to precipitate more readily, reducing the soluble calcium concentration. In contrast, in neutral and alkaline conditions, calcium remains more soluble, with its concentration increasing as the solubility of calcium compounds, like calcium carbonate, increases at higher pH levels.

Temperature changes also influence calcium concentration, as seen in Figure 10(c). At Temp. 1 (7°C), calcium is at 143 mg/L, the lowest among the temperatures. At Temp. 2 (25°C), it increases to 112 mg/L, and at Temp. 3 (36°C), it rises to 162 mg/L. The increase in calcium concentration with higher temperatures suggests that elevated temperatures enhance the solubility of calcium compounds, leading to higher concentrations of calcium in the water.

Calcium concentration fluctuates with different flow rates, as presented in Figure 10(d). At Q1 (0.5 m/h), calcium is at 153 mg/L, at Q2 (2 m/h), it decreases to 136.9 mg/L, and at Q3 (5 m/h), it rises to 183 mg/L. The increase in calcium concentration at higher flow rates can be attributed to reduced contact time between the water and the biological filter, diminishing the filter’s ability to remove calcium. Faster flow rates provide less time for calcium to precipitate or bind to other substances, leading to higher calcium concentrations in the water.

Calcium concentrations change over exposure time, as shown in Figure 10(e). At T1 (12 hours), calcium is at 185 mg/L, at T2 (24 hours), it slightly decreases to 188 mg/L, and at T3 (48 hours), it drops to 135 mg/L. This suggests that longer exposure times enhance calcium removal, likely through ion

exchange or precipitation processes. The longer the water remains in contact with the filter, the more calcium ions are removed, resulting in a lower calcium concentration over time.

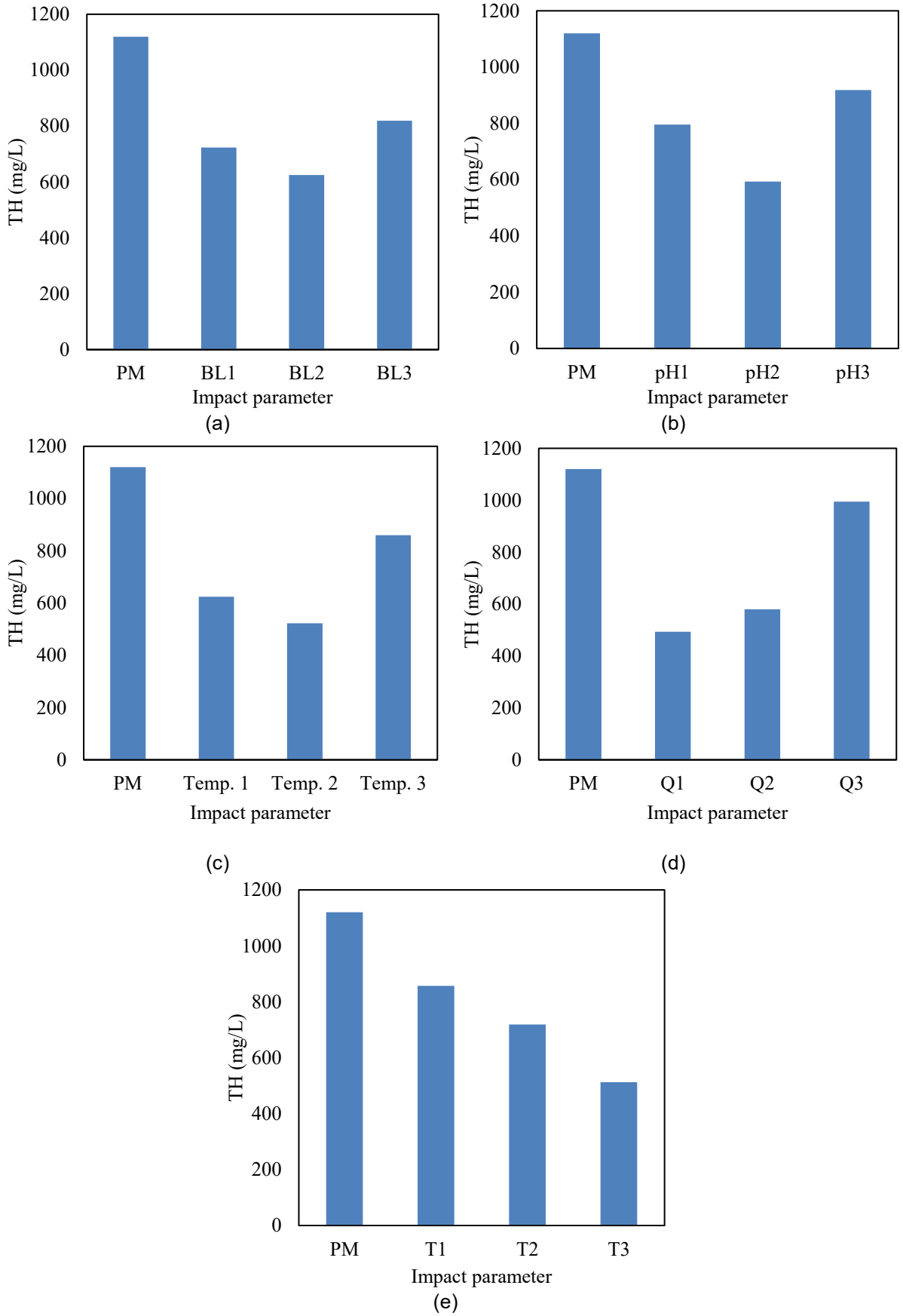

Fig. 9: Water quality parameters results under TH variation of the enhanced BSF.

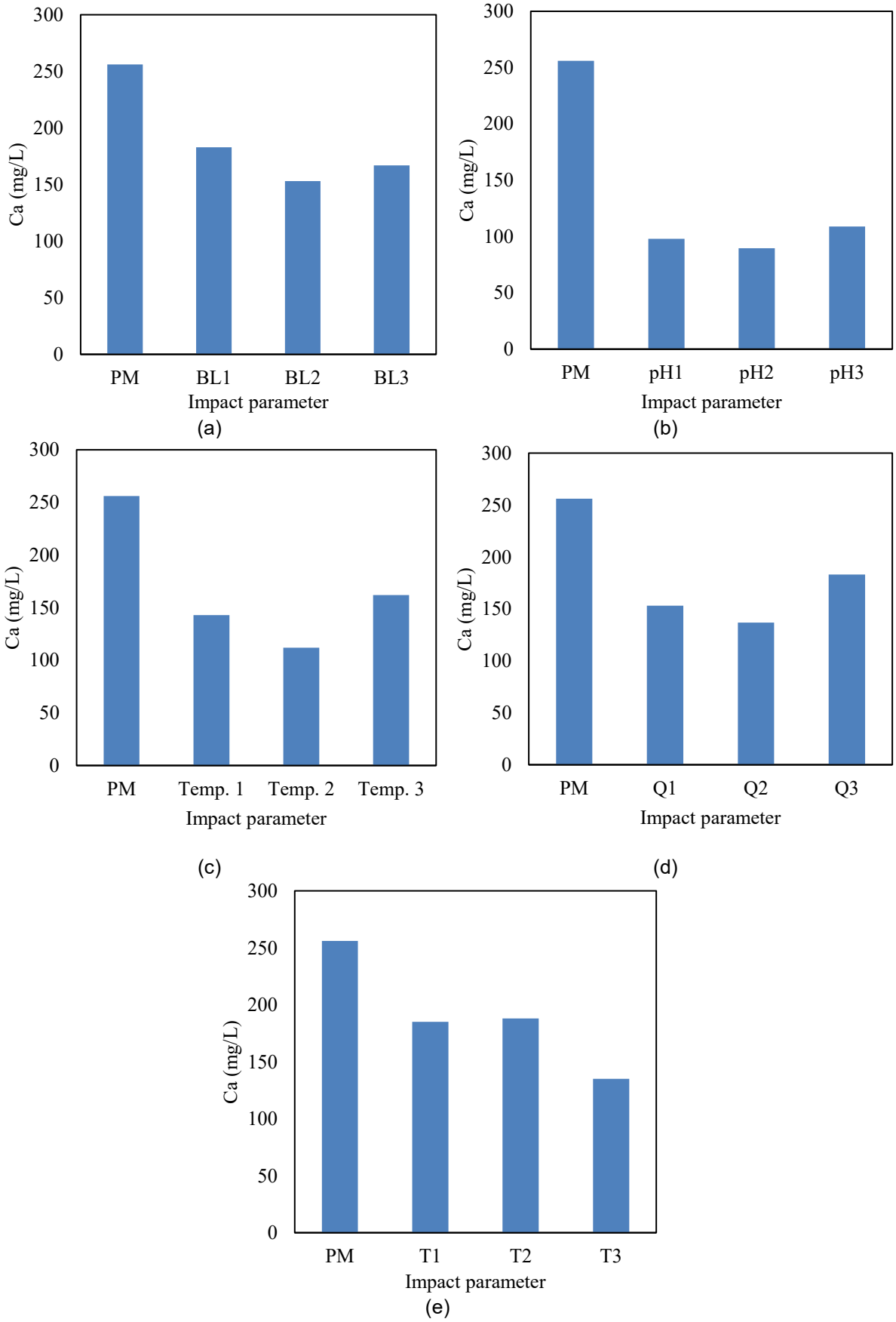

Fig. 10: Water quality parameters results under Ca variation of the enhanced BSF.

4.8 Mg variations

Magnesium (Mg) concentration shows a notable decrease with increasing biological layer thickness, as shown in Figure 11(a). At PM (Polluted Model), magnesium is at 117.2 mg/L. As the biological layer thickness increases, magnesium concentrations decrease: BL1 (1 mm) has 63 mg/L, BL2 (2 mm) has 43 mg/L, and BL3 (5 mm) has 56.7 mg/L. The general decreasing trend at BL1 and BL2 indicates that the biological layer is effective in removing magnesium. However, the increase in concentration at BL3 suggests that the layer becomes saturated at higher thicknesses, leading to reduced removal efficiency. This highlights that thinner biological layers are more efficient in removing magnesium. Magnesium concentration is also significantly influenced by pH, as shown in Figure 11(b). At pH1 (acidic, 4.01), magnesium is reduced to 93.6 mg/L. At pH2 (neutral, 6.86), it drops further to 45.16 mg/L, and at pH3 (alkaline, 9.18), it increases to 75.94 mg/L. Magnesium behaves differently across the pH range. In acidic conditions, magnesium precipitates, leading to lower concentrations, while in alkaline conditions, magnesium becomes more soluble, resulting in higher concentrations. This reflects the solubility behavior of magnesium, where it is less soluble in acidic conditions and more soluble in alkaline environments. Temperature changes also affect magnesium concentrations, as illustrated in Figure 11(c). At Temp. 1 (7°C), magnesium is at 33.46 mg/L, the lowest concentration. At Temp. 2 (25°C), it increases to 36.6 mg/L, and at Temp. 3 (36°C), it rises further to 62.7 mg/L. The increase in magnesium concentration with higher temperatures indicates that temperature enhances magnesium solubility, as higher temperatures tend to increase the dissolution rate of minerals, including magnesium. Magnesium concentration varies with flow rate, as presented in Figure 11(d). At Q1 (0.5 m/h), magnesium is at 43 mg/L. At Q2 (2 m/h), it decreases to 41 mg/L, and at Q3 (5 m/h), it increases to 102 mg/L. This trend suggests that flow rate influences magnesium removal. At higher flow rates, the contact time with the biological filter media decreases, allowing more magnesium to remain in solution. Conversely, at slower flow rates, the increased contact time facilitates magnesium precipitation or absorption, resulting in lower concentrations in the water. Magnesium concentrations change over exposure time, as shown in Figure 11(e). At T1 (12 hours), magnesium concentration is at 44 mg/L, the highest. At T2 (24 hours), it increases slightly to 47.9 mg/L, and at T3 (48 hours), it decreases to 29 mg/L. This trend suggests that longer exposure times lead to more efficient magnesium removal, likely through processes like adsorption or precipitation.

4.9 Cl variations

Chloride (Cl) concentration decreases with increasing biological layer thickness, as shown in Figure 12(a). At PM (Polluted Model), chloride concentration is 499.8 mg/L. At BL1 (1 mm), chloride is reduced to 275.6 mg/L, and at BL2 (2 mm), it drops further to 174 mg/L. However, at BL3 (5 mm), chloride concentration increases slightly to 209 mg/L. This indicates that the biological layer is effective in reducing chloride concentrations, but the reduction becomes less significant at greater layer thicknesses. The higher chloride concentration at BL3 may be due to limitations in the layer's ability to remove chloride at larger thicknesses, potentially due to increased flow rates or slower interaction with the filter media. Chloride concentration is relatively stable across different pH levels, as shown in Figure 12(b). At pH1 (acidic, 4.01), chloride concentration is 199.8 mg/L, and at pH2 (neutral, 6.86), it is 174.65 mg/L. At pH3 (alkaline, 9.18), chloride concentration increases slightly to 224 mg/L. Chloride is generally unaffected by changes in pH, showing only modest variation across the pH range. The slight increase at pH3 suggests that chloride is less sensitive to pH changes compared to other ions, maintaining a relatively stable concentration across different pH levels. Temperature has a notable effect on chloride concentration, as shown in Figure 12(c). At Temp. 1 (7°C), chloride concentration is 140.55 mg/L, the lowest observed. At Temp. 2 (25°C), it increases slightly to 134 mg/L, and at Temp. 3 (36°C), it rises significantly to 199 mg/L. This suggests that chloride solubility increases with temperature, with higher temperatures leading to higher concentrations. The decrease at Temp. 2 could indicate that other processes, such as precipitation or adsorption, are reducing chloride levels before the temperature rises further. Chloride concentration also varies with flow rate, as presented in Figure 12(d). At Q1 (0.5 m/h), chloride concentration is 164.68 mg/L. At Q2 (2 m/h), the concentration decreases slightly to 149.86 mg/L, but at Q3 (5 m/h), it increases to 188 mg/L. This trend indicates that slower flow rates allow for more interaction with the filter media, leading to better chloride removal. In contrast, higher flow rates reduce the contact time with the filter media, allowing more chloride to remain in the water. The increase at Q3 suggests that higher flow velocities may pose challenges in removing chloride effectively. Chloride concentration also varies with exposure time, as shown in Figure 12(e). At T1 (12 hours), chloride concentration is 216.4 mg/L. At T2 (24 hours), it decreases to 183 mg/L, and at T3 (48 hours), it further drops to 136 mg/L. This indicates that longer exposure times facilitate better chloride removal, likely

through processes like adsorption onto particulate matter or filtration media. The system's chloride removal efficiency improves over time as it interacts more with the water.

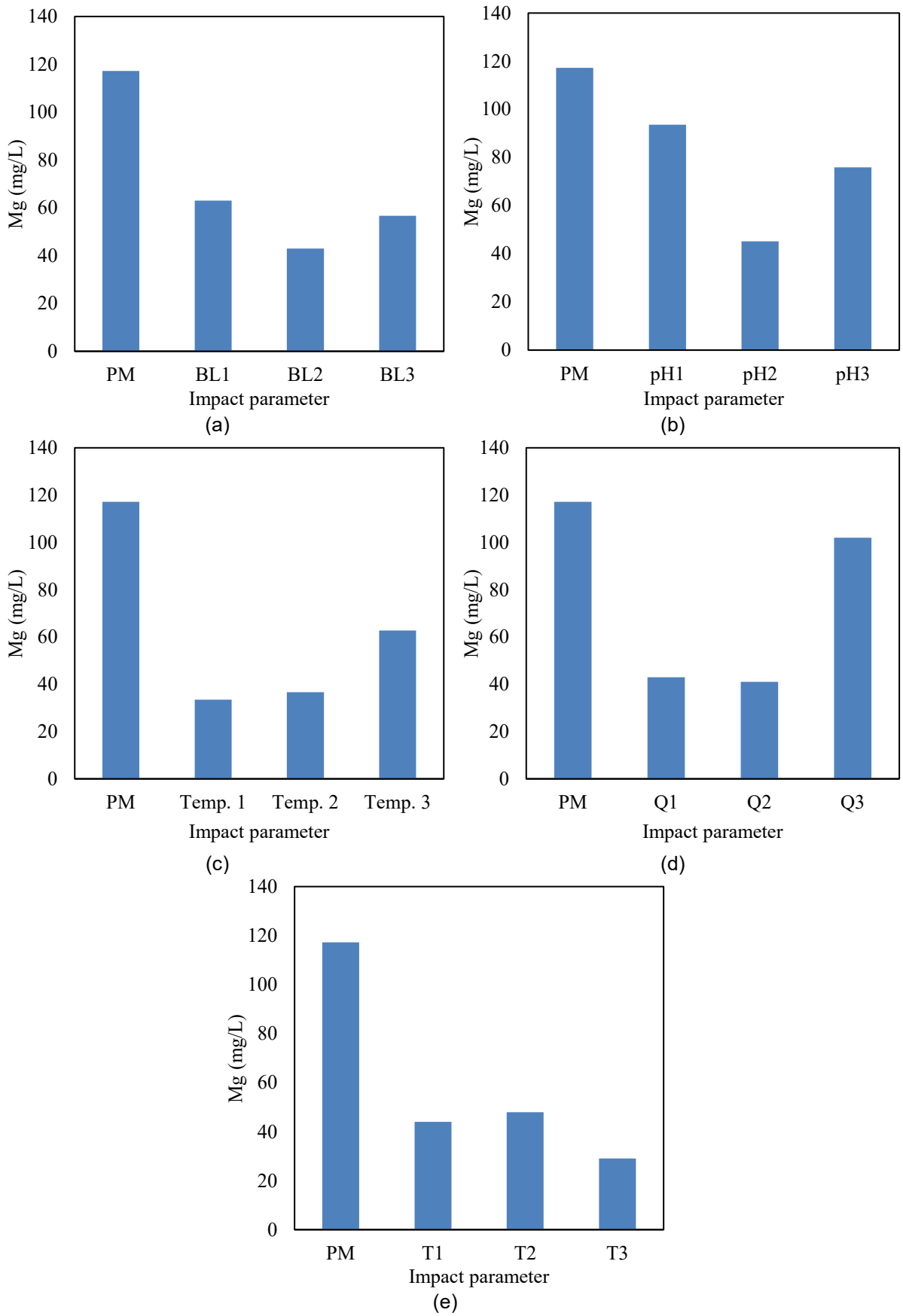

Fig. 11: Water quality parameters results under Ca variation of the enhanced BSF.

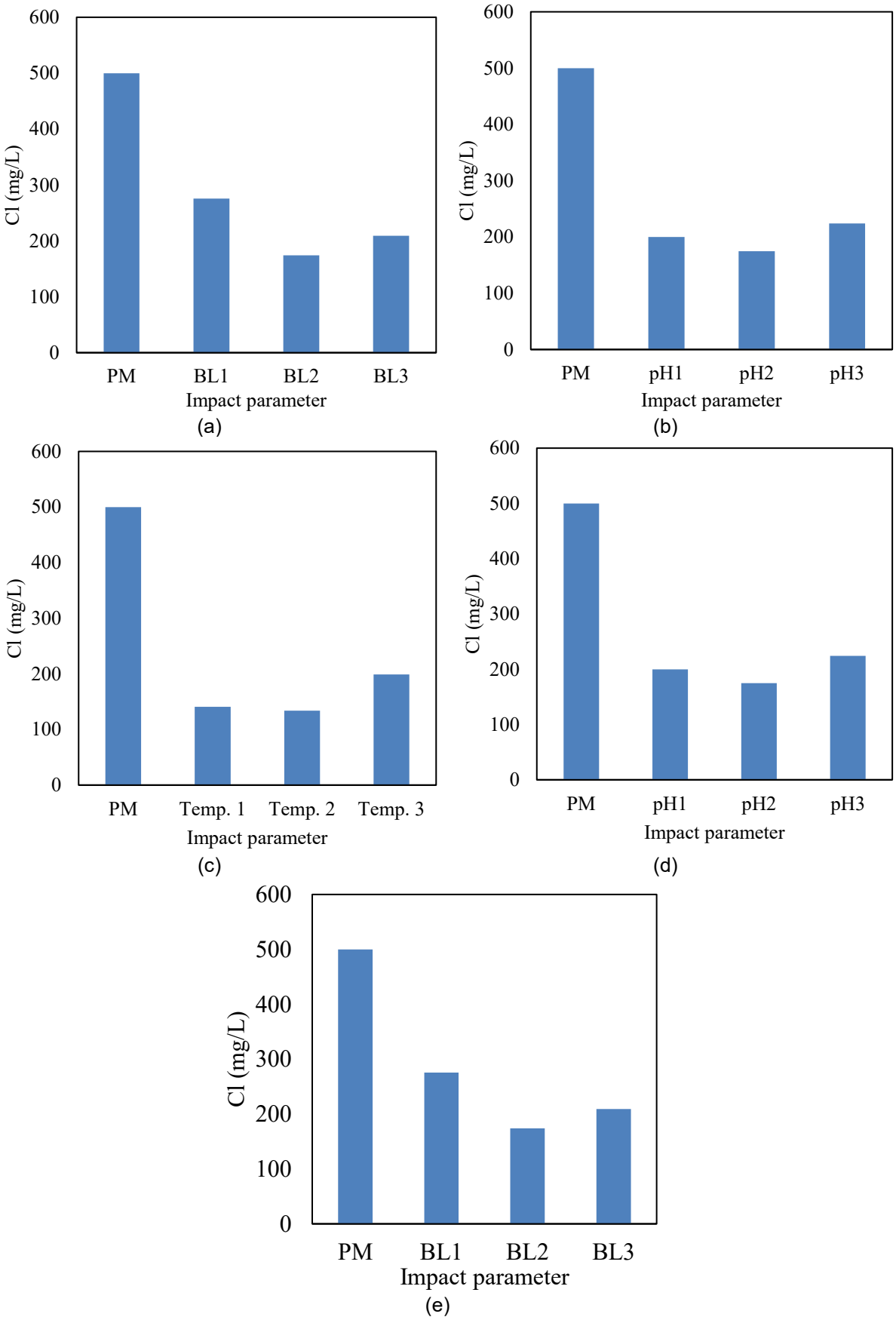

Fig. 12: Water quality parameters results under Cl variation of the enhanced BSF.

4.10 So_4 variations

Sulfate (SO_4) concentration decreases as the biological layer thickness increases, similar to chloride but with less drastic reduction, as presented in Figure (13 a). At PM (Polluted Model), sulfate concentration is 827.63 mg/L. At BL1 (1 mm), it reduces to 488 mg/L, and at BL2 (2 mm), it further decreases to 455.19 mg/L. At BL3 (5 mm), the concentration is 483.7 mg/L, indicating that the biological layer still plays a significant role in reducing sulfate concentrations, although the rate of reduction diminishes with the increasing thickness of the layer.

Sulfate concentration responds moderately to pH changes, as shown in Figure (13 b). At pH1 (acidic, 4.01), sulfate concentration is 461.6 mg/L. At pH2 (neutral, 6.86), it decreases to 389.45 mg/L. At pH3 (alkaline, 9.18), the sulfate concentration increases to 478 mg/L. This suggests that the solubility and mobility of sulfate may vary slightly across different pH values, with a lower concentration at pH2 (neutral) and a slightly increased concentration under more alkaline conditions (pH3). The pH effect on sulfate concentration is less pronounced compared to other ions like chloride, but it still shows some influence, particularly at extreme pH values. Sulfate concentration follows a similar pattern to chloride, see Figure (13 c), with noticeable changes across varying temperature conditions. At Temp. 1 (7°C), sulfate concentration is 409.77 mg/L. At Temp. 2 (25°C), it rises slightly to 420 mg/L, and at Temp. 3 (36°C), it increases further to 499 mg/L. The increase in sulfate concentration with temperature suggests that sulfate solubility increases with temperature, a common characteristic for many dissolved ions. The higher concentration at Temp. 3 may indicate a greater dissolution of sulfate into the water at higher temperatures, which is important to consider in warmer water environments where sulfate levels may spike. Flow rate shows an interesting trend in sulfate concentration, as presented in Figure (13 d). At Q1 (0.5 m/h), sulfate concentration is 422 mg/L. At Q2 (2 m/h), it decreases slightly to 414 mg/L, and at Q3 (5 m/h), it rises to 517.4 mg/L. This trend suggests that lower flow rates provide more time for sulfate interaction with the water treatment system, leading to a reduction in concentration. However, as the flow rate increases, there may be less contact time, which allows more sulfate to remain in the water. The sharp increase at Q3 indicates that very high flow rates reduce sulfate removal efficiency, which is critical in designing water treatment systems to ensure proper contact time for effective removal.

Sulfate concentration decreases over time, see Figure (13 e), with T1 (12 hours) at 506 mg/L, T2 (24 hours) at 494 mg/L, and T3 (48 hours) at 420 mg/L. This shows that as exposure time increases, sulfate concentration tends to decrease, likely due to processes such as adsorption, filtration, or chemical reactions with the treatment media.

4.11 E.coli variations

E. coli concentrations decrease significantly as the biological layer thickness increases, as presented in Figure (14 a). At PM, the E. coli concentration is 85 CFU/100mL. At BL1 (1 mm), the concentration decreases to 43 CFU/100mL, and it continues to decrease at BL2 (2 mm), with a concentration of 16 CFU/100mL. Finally, at BL3 (5 mm), the concentration drops further to 7 CFU/100mL. This trend suggests that the biological layer is effective in reducing E. coli levels, likely through biological filtration or adsorption processes.

E. coli concentration shows a marked decrease with changes in pH, as shown in Figure (14 b). At pH1 (acidic, 4.01), the concentration is 5 CFU/100mL. At pH2 (neutral, 6.86), it is even lower at 2 CFU/100mL. At pH3 (alkaline, 9.18), the concentration increases slightly to 13 CFU/100mL. The decrease in concentration at acidic and neutral pH suggests that lower pH values may be more effective in reducing E. coli numbers, likely due to the inhibitory effects of acidic conditions on bacterial survival and growth. The slight increase in concentration under alkaline conditions (pH3) may indicate that more favorable conditions for bacterial survival exist at higher pH levels. Temperature has a notable impact on E. coli concentrations. At Temp. 1 (7°C), the concentration is 9 CFU/100mL, as presented in Figure (14 c). As temperature increases to Temp. 2 (25°C), the concentration decreases significantly to 2 CFU/100mL, and at Temp. 3 (36°C), it further decreases to 7 CFU/100mL. The higher temperature of Temp. 2 seems to favor a reduction in E. coli levels, possibly due to the greater activity of disinfectant processes or temperature-sensitive bacteria. However, at Temp. 3, the increase in concentration could be due to the potential resurgence of E. coli or a reactivation of dormant bacteria under warmer conditions. E. coli concentrations change with different flow rates, see Figure (14 d). At Q1 (0.5 m/h), the concentration is 1 CFU/100mL. At Q2 (2 m/h), the concentration increases to 4 CFU/100mL, and at Q3 (5 m/h), it rises to 25 CFU/100mL. The exposure time also plays a significant role in the removal of E. coli. At T1 (12 hours), the concentration is 1 CFU/100mL, and it remains the same at T2 (24 hours). At T3 (48 hours), the concentration drops to 0 CFU/100mL, as presented in Figure (14 e). This trend

demonstrates that extended exposure times significantly contribute to the reduction of E. coli, likely due to the prolonged effect of disinfection or bacterial adsorption processes over time.

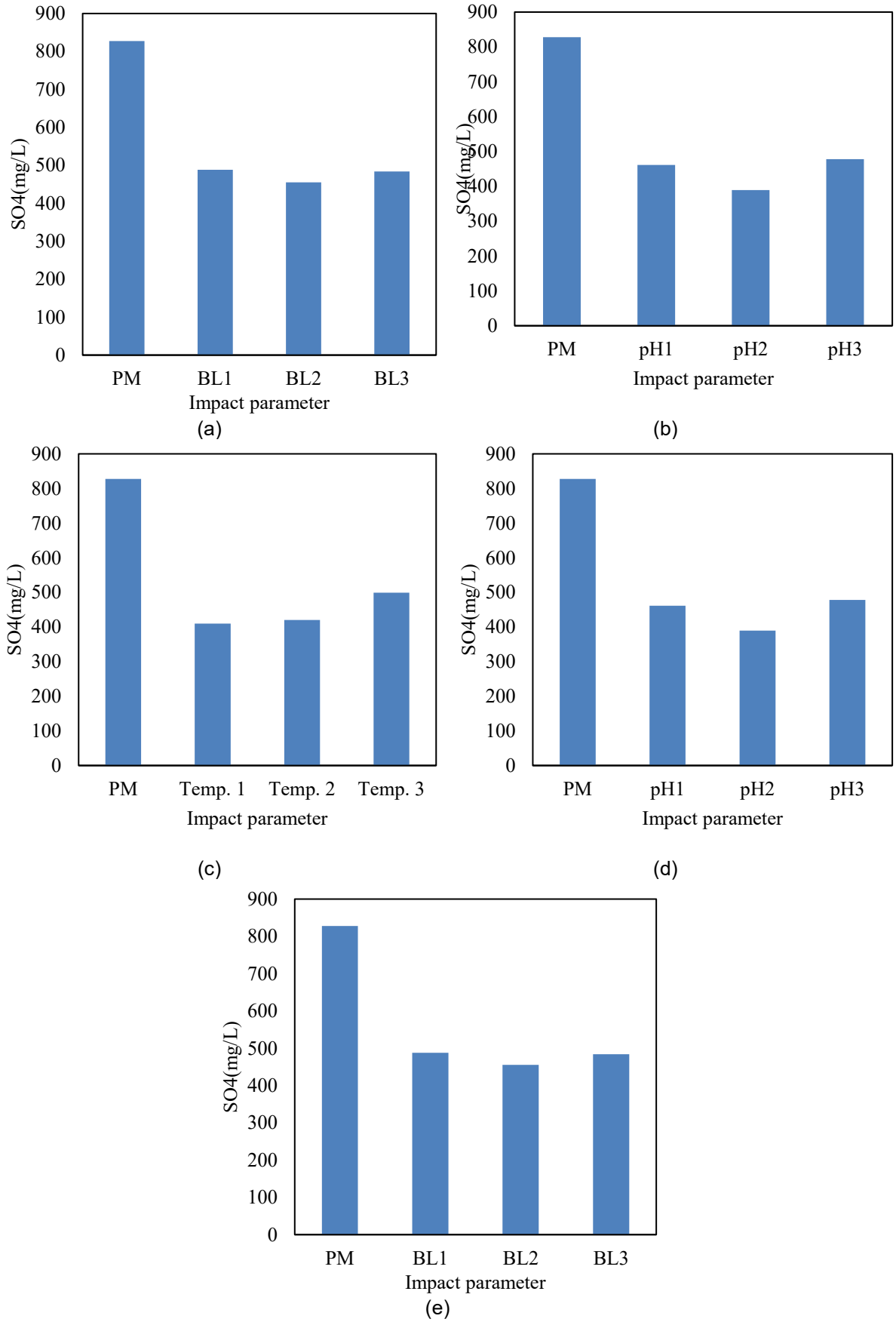

Fig. 13: Water quality parameters results under So_4 variation of the enhanced BSF.

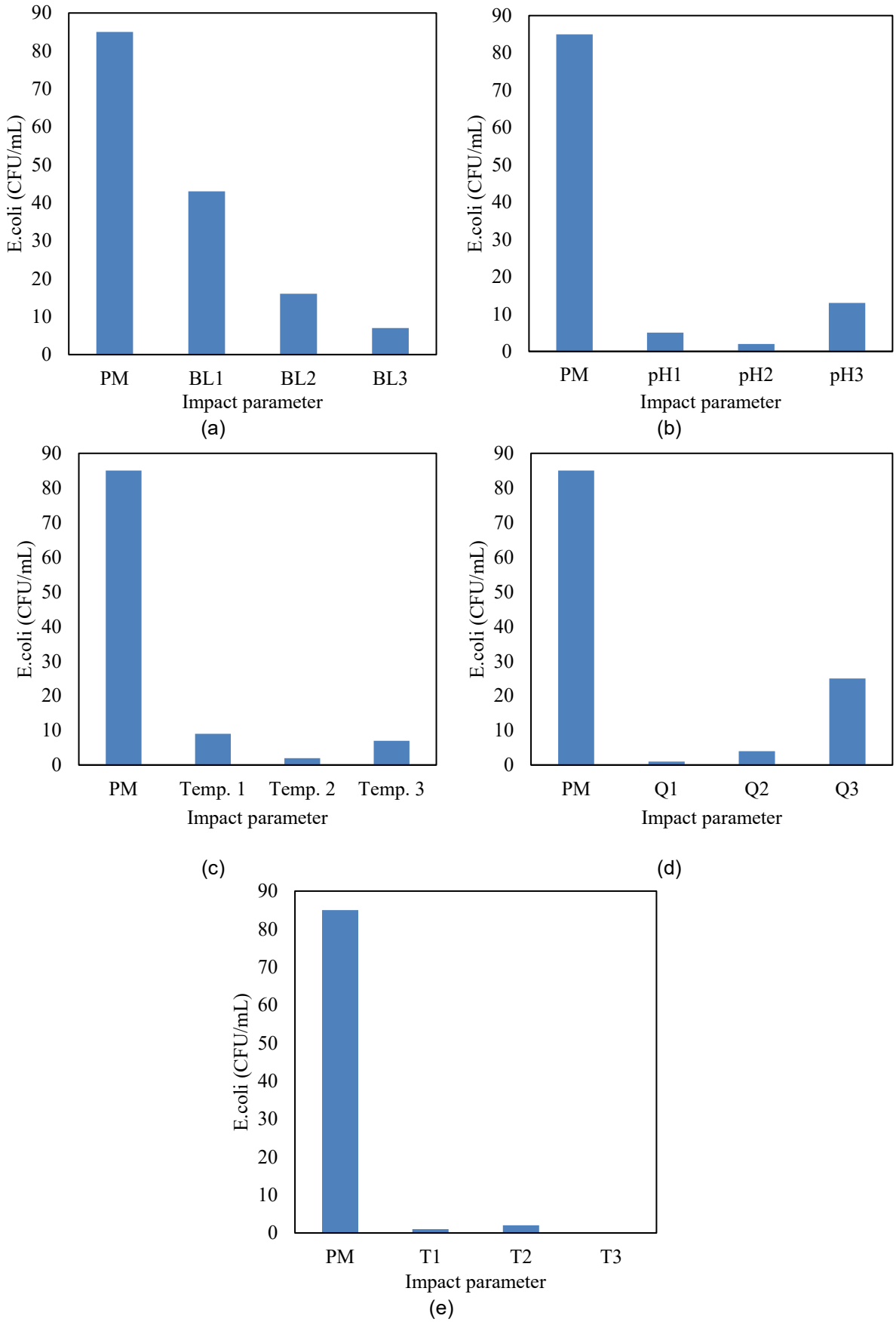

Fig. 14: Water quality parameters results under E.coli variation of the enhanced BSF.

The removel effeciency results indicate that different contaminants respond best under varying conditions, as shown in Fig. (15) and Table (3). However, a few key trends emerge in microbial contaminant removal, suspended solids reduction, dissolved solids and conductivity, hardness reduction, and chloride and sulfate removal.

The highest E. coli removal (100%) occurred at a 48-hour retention time, demonstrating that prolonged exposure is crucial for eliminating microbial contaminants. The biological layer (2 mm) played a significant role, removing over 81.2% of bacteria, suggesting that biofilm formation enhances pathogen reduction.

For suspended solids and turbidity reduction, the best removal was achieved at a 0.5 m/h flow rate, leading to an 85.4% decrease in turbidity. The biological layer (2 mm) significantly contributed to filtering fine particles, indicating its effectiveness in reducing suspended matter.

Dissolved solids and conductivity removal were optimal at pH 4.01, likely due to enhanced chemical interactions at low pH levels. TDS decreased by 65.4%, while EC was reduced by 56.9%, demonstrating the impact of pH control on filtration efficiency and ion exchange mechanisms. Hardness reduction varied with temperature and pH conditions. Total hardness (TH) showed the highest reduction (53.3%) at 25°C, while Calcium (Ca) was best removed at pH 4.01 (61.7%). Magnesium (Mg) exhibited the most significant decrease (75.2%) at a 48-hour retention time, highlighting the importance of both pH and contact duration in hardness reduction.

For chloride and sulfate removal, chloride (Cl) showed the highest reduction (73.2%) at 25°C, suggesting that temperature plays a crucial role in ion exchange and adsorption. Sulfate (SO_4) removal was most effective at pH 6.86 (52.9%), indicating that a neutral pH environment optimizes sulfate reduction mechanisms. These findings emphasize the importance of adjusting pH, retention time, flow rate, and biological filtration layers to maximize removal efficiency across different contaminants.

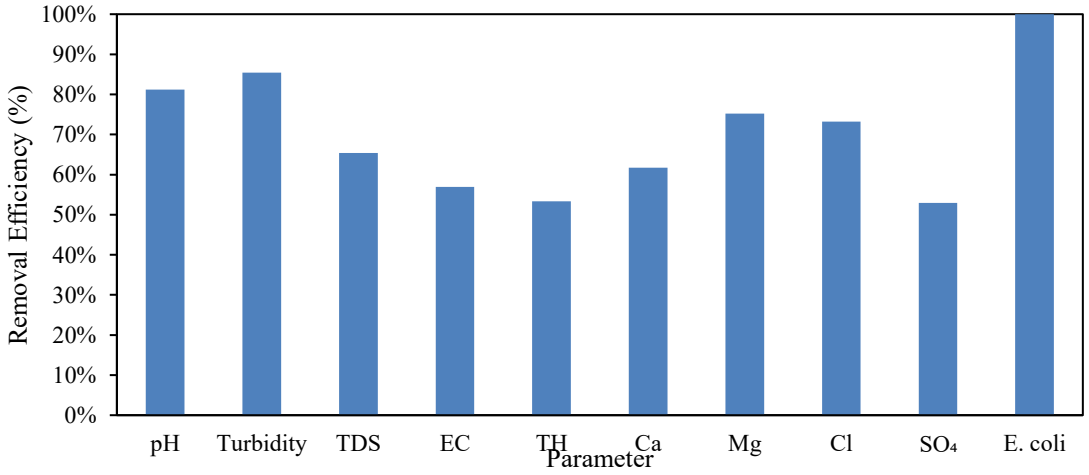

Fig. 15: Removel effeciency of each parameter during BSF experiments.

Table 4. Removel efficiency of each contamenent.

Parameter	Initial Value	Final Value	Best Condition for Maximum Removal	Removal Efficiency [%]
pH	4.01 - 9.18	4.0 - 9.3	pH 6.86 for optimal removal	81.2%
Turbidity	13.7	2	0.5 m/h flow rate	85.40%
TDS	1761.5	609	pH 4.01	65.40%
EC	2710	1167	pH 4.01	56.90%
TH	1120	523	25°C	53.30%
Ca	256	98	pH 4.01	61.70%
Mg	117.2	29	48-hour retention time	75.20%
Cl	499.8	134	25°C	73.20%
SO_4	827.63	389.45	pH 6.86	52.90%
E. coli	85	0	48-hour retention time	100%

5 Conclusion

This study demonstrates the effectiveness of a Cane Papyrus-enhanced biosand filter (BSF) for improving water quality through optimized operational conditions. The main conclusions are as follows:

1) A 48-hour retention time achieved complete (100%) E. coli removal, highlighting the critical role of sufficient contact time in microbial inactivation.

2) The presence of a 2 mm biological layer significantly enhanced contaminant removal, particularly by supporting biofilm development essential for pathogen reduction and suspended solids filtration.

3) A flow rate of 0.5 m/h provided the highest reduction in suspended solids and turbidity (85.4%), emphasizing that lower flow rates favor better physical filtration performance.

4) Acidic conditions (pH 4.01) improved the removal of Total Dissolved Solids (65.4%) and Electrical Conductivity (56.9%), suggesting enhanced chemical interaction and ion exchange under low pH environments.

5) Optimal temperature conditions (25°C) supported the greatest reductions in Total Hardness (53.3%) and Chloride (73.2%) concentrations, while Magnesium removal (75.2%) was maximized at a 48-hour retention time, and Sulfate removal was best at neutral pH (6.86).

6) The findings emphasize that tailoring BSF operational parameters—such as pH, retention time, flow rate, and biofilm development, to target specific contaminants can significantly improve overall treatment performance, offering practical, low-cost water purification options for communities in need.

The findings underscore the critical role of optimizing operational parameters, such as pH, retention time, flow rate, and biological filtration layers, to maximize contaminant removal efficiency in BSF systems. Tailoring these parameters to specific contaminant types can significantly enhance the treatment performance of BSF systems, making them more effective for diverse water treatment applications. Future studies are recommended to explore long-term performance, larger-scale applications, and comparative evaluations with other natural media to further enhance the practical application of the system.

Conflict-of-Interest

There are no conflicts of interest to declare.

References

[1] ANDREOLI, F. C., & SABOGAL-PAZ, L. P. (2020). Household slow sand filter to treat groundwater with microbiological risks in rural communities. Water Research, 186, 116352.

[2] BACHAR, N., LINDENSTRAUSS, N., DAVID, S., MIRKIN, M., POLANI, N., GUETA, O., ... & RONEN, A. (2024). Improving Water Quality by Combined Sedimentation and Slow Sand Filtration: A Case Study in a Maasai Community, Tanzania. Applied Sciences, 14(20), 9467.

[3] WEBSTER, T. M., & FIERER, N. (2019). Microbial dynamics of biosand filters and contributions of the microbial food web to effective treatment of wastewater-impacted water sources. Applied and Environmental Microbiology, 85(17), e01142-19.

[4] KISAKYE, V. (2023). A bucket sand filter and Moringa oleifera drinking water treatment hybrid system for rural households. Scientific African, 20, e01689.

[5] SABER, Q.A., ALSULTANI, R., AL-SAADI, A.A., KARIM, I.R., KHASSAF, S.I., MOHAMMED, O.I., ABED, S.M., NASER, R.A., HUSSEIN, A., MUSLIM, F., NAIMI, S., SALAHALDAIN, Z. (2025). Structural finite element analysis of bridge piers with consideration of hydrodynamic forces and earthquake effects for a sustainable approach. Mathematical Modelling of Engineering Problems, Vol. 12, No. 3, pp. 1071-1080. https://doi.org/10.18280/mmep.120334.

[6] MYAN, H. (2014). Effective Used of Bio-Cement Jar BSF in Rainwater Harvesting System. In Symposium on Mainstreaming Rainwater Harvesting as a Water Supply Option (p. 26).

[7] SHOLLENBERGER, H., MATHEWS IV, G., YOUNG, M., CLARK, S., & CHEN, Y. (2023). A solar radiation and biosand filtration system for cooking and water treatment. International Journal of Environmental Science and Technology, 20(6), 5983-5994.

[8] OBEID, A. F., NILE, B. K., & FAROUK, M. (2024). Sulfate removal from wastewater by using waste material as an adsorbent. Open Engineering, 14(1), 20220532.

[9] DANLEY, A. A., HUANG, E. C., WORLEY-MORSE, T., & GUNSCH, C. K. (2018). Evaluating the role of total organic carbon in predicting the treatment efficacy of BSFS for the removal of Vibrio cholerae in drinking water during startup. Journal of applied microbiology, 125(3), 917-928.

[10] MUTEMI, S., HOKO, Z., & MAKURIRA, H. (2020). Investigating feasibility of use of bio-sand filters for household water treatment in Epworth, Zimbabwe. Physics and Chemistry of the Earth, Parts A/b/c, 117, 102864.
[11] ENIOLA, J. O., & SIZIRICI, B. (2023). Investigation of biochar-modified biosand filter performance for groundwater treatment for drinking water purposes: A laboratory and pilot scale study. Journal of Water Process Engineering, 53, 103914.
[12] ENIOLA, J. O., & SIZIRICI, B. (2024). Assessing the sustainability of modified biosand filters using life cycle assessment, cost and performance factors. Environment, Development and Sustainability, 1-25.
[13] WELZ, P. J. (2024). Biosand Reactors for Municipal and Industrial Wastewater Treatment: Status Quo, Challenges and Opportunities. Processes, 12(4), 641.
[14] AFAN, H. A., MOHTAR, W. H. M. W., KHALEEL, F., KAMEL, A. H., MANSOOR, S. S., ALSULTANI, R., ... & EL-SHAFIE, A. (2024). Data-driven water quality prediction for wastewater treatment plants. Heliyon, 10(18). https://doi.org/10.1016/j.heliyon.2024.e36940
[15] ABDIYEV, K., AZAT, S., KULDEYEV, E., YBYRAIYMKUL, D., KABDRAKHMANOVA, S., BERNDTSSON, R., ... & SULTAKHAN, S. (2023). Review of slow sand filtration for raw water treatment with potential application in less-developed countries. Water, 15(11), 2007.
[16] MULUGETA, S., HELMREICH, B., DREWES, J. E., & NIGUSSIE, A. (2020). Consequences of fluctuating depth of filter media on coliform removal performance and effluent reuse opportunities of a bio-sand filter in municipal wastewater treatment. Journal of Environmental Chemical Engineering, 8(5), 104135.
[17] EMSLIE, D., SIDDIQUA, S., CRAWFORD, B., & TEECE, W. (2021). Biofilm formation and effectiveness of biosand filtration systems with typical and innovative filter media. Geotechnical and Geological Engineering, 1-16.
[18] DANDADZI, P., & KOTHURKAR, N. K. (2023). Assessing the sustainability of biosand filters: Unveiling interlinkages and leveraging factors for effective implementation. Environmental and Sustainability Indicators, 100311.
[19] GANESAN, S., DANGRIT, S., & JANJAROEN, D. (2023). Long-term arsenate removal by an iron-amended biosand filter: Modes of operation according to groundwater composition. Journal of Environmental Chemical Engineering, 11(3), 109814.
[20] SHARMA, P., DAR, M. U. D., & KUSHWAHA, N. L. (2023). Biosand Filters for Household Wastewater Treatment. In Advanced Technologies for Water Quality Treatment and Management (pp. 185-199). Apple Academic Press.
[21] MAHMOOD, P., KHAN, A. H., HAIDER, S., SYED, Z., KHALIQ, M., & ZAHEER, S. (2024). Application of Bio Sand Filters for improving drinking water quality in flood-affected areas of Pakistan, a case study of Shahdad Kot, Pakistan. Case Studies in Chemical and Environmental Eng., 9, 100769.
[22] TSAFACK, H. N., DJOKO, G. R. P., AKWA, T. E., KWEKAP, J. W., WAMBA, F. R., & TEMGOUA, E. (2024). Assessment of filtration capacity of different filters used in the West Region of Cameroon for quality improvement of drinking water. Sustainable Water Resources Management, 10(4), 159.
[23] JOUDAH, Z. H., HAFIZAH A. KHALID, N., ALGAIFI, H. A., MHAYA, A. M., XIONG, T., ALSULTANI, R., & HUSEIEN, G. F. (2024). Effects of Waste Glass Bottle Nanoparticles and High Volume of Waste Ceramic Tiles on Concrete Performance When Exposed to Elevated Temperatures: Experimental and Theoretical Evaluations. Fire, 7(12), 426. https://doi.org/10.3390/fire7120426.
[24] NITHTHIYARAJA, K., HETTITHANTHRI, O., & VITHANAGE, M. (2025). Biochar Filters and Its Application in Drinking Water Treatment. In Biochar Amendments for Environmental Remediation (pp. 337-346). CRC Press.
[25] OBEID, A. F., NILE, B. K., & AL JUBOURY, M. F. (2023). Adsorption Sulfate from Wastewater by Using New Material. In E3S Web of Conferences (Vol. 427, p. 04003). EDP Sciences.
[26] ELEMO, T., CHIPPS, M., GRAHAM, N., TURNER, A., BRETAGNE, S., JEFFERSON, B., & HASSARD, F. (2025). Evaluating the impact of underwater skimming on slow sand filter performance and operation. Water Research, 123234.
[27] ALSULTANI R, SABER Q, AL-SAADI A, MOHAMMED O, ABED S, NASER R, HUSSEIN A, MUSLIM F, FADHIL H, KARIM I, KHASSAF S. The Impact of Climate Change on the Reinforcement Durability of Concrete Bridge Structures. Open Civ Eng J, 2024; 18: e18741495337012. http://dx.doi.org/10.2174/0118741495337012240812105905
[28] SARAVANAN, S. P., & GOBINATH, R. (2015). Drinking Water safety through bio sand filter-A case study of Kovilambakkam Village, Chennai. International Journal of Applied Engineering Research, 10(53), 254-262.

[29] AL JUBOURY, M. F., ABDULREDHA, M., & NILE, B. K. (2022). Photocatalysis and flocculation processes for recycling aquaculture effluent into irrigation water. Water Supply, 22(3), 3103-3113.
[30] MAGEED, N. N., ALSULTANI, R., & ABBAS, A. W. N. (2024). The Impact of Using Advanced Technologies in Sustainable Design to Enhance Usability and Achieve Optimal Architectural Design. International Journal of Sustainable Development & Planning, 19(11). https://doi.org/10.18280/ijsdp.191116
[31] RAHMADYANTI, E., & PALUPI, A. E. (2025). Rainwater treatment with bio-slow sand filtration for sustainable water supply. Journal of Ecological Engineering, 26(2).
[32] SHEHAB, E. Q., & ALSULTANI, R. (2025). A new approach to sustainable environmental assessment for wastewater treatment plants-A case study in the central region of Iraq. Ecological Engineering & Environmental Technology (EEET), 26(1). https://doi.org/10.12912/27197050/194126.
[33] MULAY, B. N., & REDDY, K. R. (2021). Study of biofilter planted with basil for removal of ammonia in aquaponic water. Civil and Environmental Engineering, 17(1), 242-251.
[34] ALSULTANI, R., KARIM, I. R., & KHASSAF, S. I. (2025). Experimental and numerical investigation into pile spacing effects on the dynamic response of coastal pile foundation bridges considering current-wave-earthquake forces. Advances in Bridge Engineering, 6(1), 1. https://doi.org/10.1186/s43251-024-00147-z
[35] JASSAM, M. G., ABD, A. H., & HUSSEIN, M. A. (2023). Effect of Initial Water Content on the Collapsibility of Natural and Cement-Treated Gypseous Soils. Civil And Environmental Engineering Reports, 19(2), 610-617.